Project Narrative
Cover Page

Company Name & Address:	Particle Beam Lasers, Inc. 18925 Dearborn Street Northridge, CA 91324-2807
Principal Investigator:	Robert J. Weggel
Project Title:	Development of Open-Midplane Dipole Magnets For Muon Accelerators
DOE Grant Number:	DE-SC0004494
Topic No: 64	Advanced Concepts and Technology for High Energy Accelerators
Subtopic: (b)	Technology for Muon Colliders and Muon Beams

Identification and Significance of the Problem or Opportunity, and Technical Approach

1. Scientific Case for Muon Accelerators and $\mu^+\mu^-$ Colliders

The national Muon Acceleration Program (MAP) has recently been approved by the U.S. Department of Energy [1]. A key R&D component within the program is the development of the technology required to cope with radiation from the decay of muons circulating within the accelerator or storage rings. Studies of magnet systems near the interaction regions (IR) of the collider have been underway at FNAL, and progress has been reported [2]. In this proposal, we focus on the mitigation of dispersed power along the magnets within the arcs of the rings.

The concept of a muon collider was revived at a workshop in Napa, CA in 1992 [3, 4] and studied in subsequent workshops [3]. A collider that uses muons instead of electrons can recirculate particles and therefore can be more compact and less costly in RF than a linear collider. The recent P5 committee has strongly endorsed the study of a muon collider, as has the Muon Accelerator Program (MAP).

The physics motivation is strong for a muon collider. One of low energy could produce millions of Higgs bosons for study. One of high energy—say 1.5 TeV—could build upon the discoveries at the LHC to refine understanding of the new particles [4]. Polarized muons could be used [3]. A muon accelerator also can be a neutrino factory. A schematic of both machines is shown in Fig. 1, extracted from the muon collider task force document.

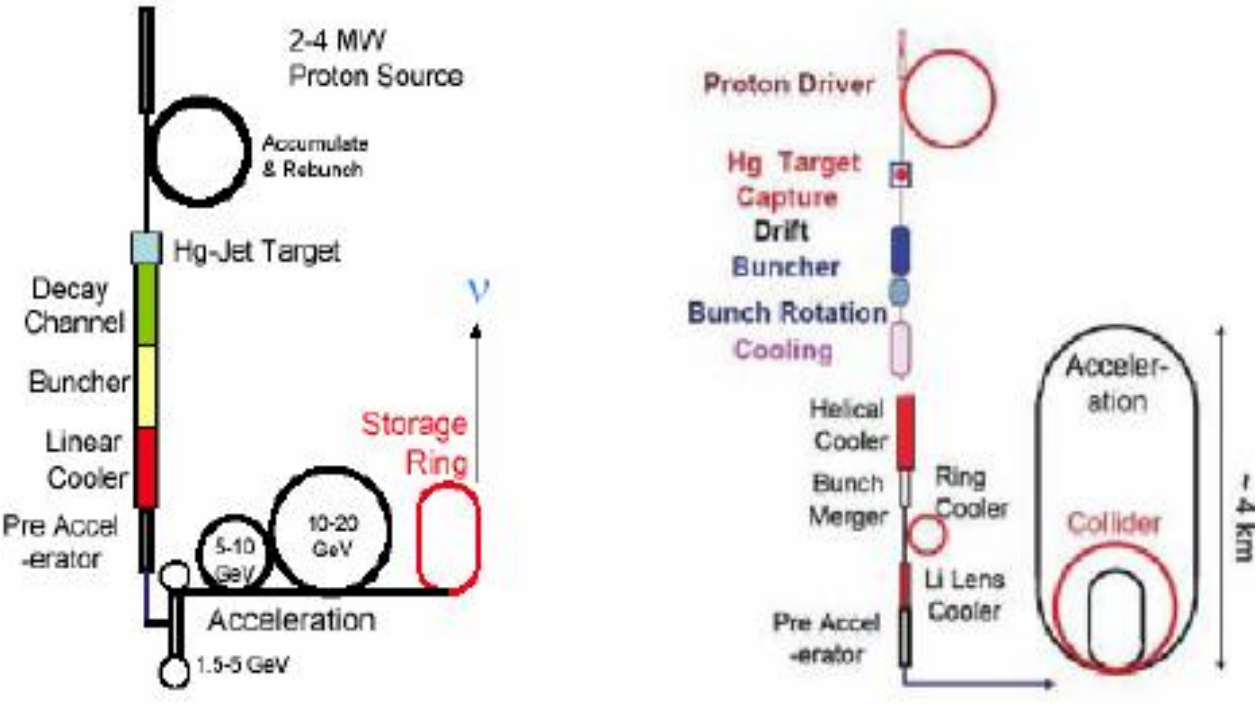

Fig. 1. Schematic of muon accelerators. Left: A neutrino factory; Right: A muon collider.

A muon collider is technically extremely challenging. It needs many orders of magnitude of six-dimensional cooling of the $\mu^{\pm}$ to achieve the very low emittance required for high luminosity; 6-D cooling has yet to be demonstrated. However, many new ideas are being pursued, and the Muon Ionization Cooling Experiment (MICE) at RAL (Rutherford Appleton Laboratory) will soon test transverse cooling.

An additional challenge is radiational heating from muon decay, via $\mu^{\pm} \rightarrow e^{\pm} + \nu + \bar{\nu}$, of the $\sim 10^{12}$ muons in the ring. The heating can be so intense as to quench the superconducting dipoles that steer the muon beam [3]. To shield the magnets from the radiation is expensive, because the magnet bore must be very large to accommodate enough shielding (Fig. 2a). An alternative is to design the magnet to have no conductor near the plane of the accelerator or storage ring, where most of the muon decay takes place. This is the concept of the open-midplane dipole (OMD) magnet (Fig. 2b). Structural analysis in Phase I of this SBIR has tended to confirm that open-midplane dipoles should be feasible to at least 10 T with Nb_3Sn and perhaps to 20 T with high-temperature superconductors (HTS)—either BSCCO (bismuth strontium calcium copper oxide) or YBCO (yttrium barium copper oxide)—wherever demanded by the intensity of the ambient field or the energy deposition. HTS is appealing not only for its field capability but also for its radiation tolerance (likely long-term as well as short-term).

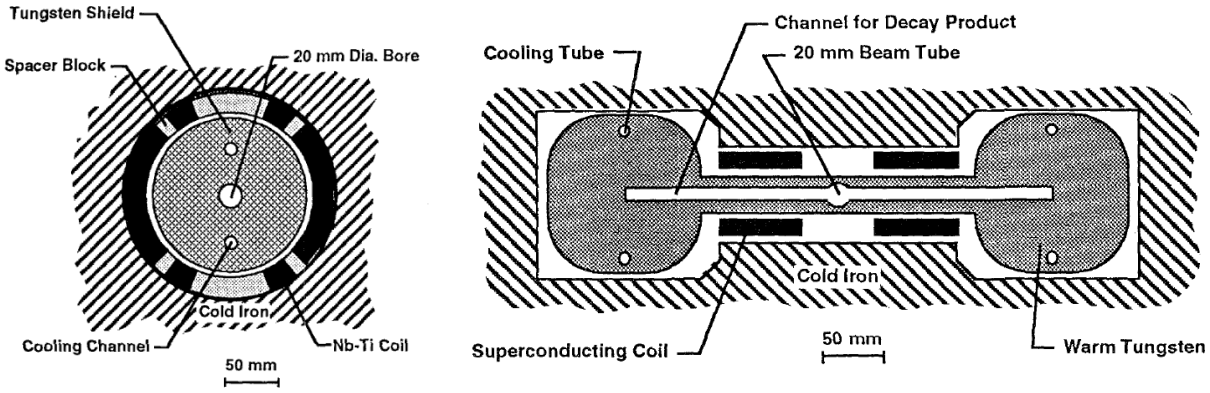

Figs. 2a & b. Dipole magnets for muon accelerators and colliders. Left: Cosine theta magnet with tungsten absorber 65 mm thick. Right: The open-midplane dipole of Nucl. Phys. B, 51A, 1996, p. 166, with superconducting-coil heat load less than 0.1% that from the muon decay.

2. Current Understanding of the Muon Collider Lattice

In 1995 the first study of the lattice of a muon collider was carried out by A. Garren, et al. [3]; Table 1 summarizes its parameters. M. Green—then of LBNL (Lawrence Berkeley National Laboratory)—designed an appropriate dipole magnet [5]. It required a thick layer of tungsten to shield the coils from the muon-decay radiation and beam halo. Therefore he suggested a novel geometry to dodge much of the beam debris—the open-midplane design [5]. This geometry was examined also by McIntyre, et al. for a somewhat higher field magnet [6] and later by Parker, Gupta, et al. [7].

Table 1. First Study of a Lattice for a $\mu^+\mu^-$ Collider (A. Garren, et al., 1995)

High-Energy/High-Luminosity $\mu^+\mu^-$ Collider (Nuclear Physics B, 51A, 1996, p. 149)	
Maximum c-of-m energy [TeV]	4
Luminosity L [10^{35}cm^{-2} s^{-1}]	1.0
Circumference [km]	8.08
Time between collisions [μs]	12
Energy spread σ_e [units 10^{-3}]	2
Pulse length σ_x [mm]	3
Free space at the IP [m]	6.25
Luminosity lifetime [No. of turns]	900
rms emittance $\varepsilon_{x,y}^N$ [10^{-6} m·rad]	50.0
rms emittance $\varepsilon_{x,y}$ [10^{-6} m·rad]	0.0026
Beta function at IP, β* [mm]	3
rms beam size at IP [μm]	2.8
Quadrupole pole fields near IP [T]	6.0
Maximum beta function, β_{max} [km]	400
Magnet aperture closest to IP [cm]	12
Beam-beam tune shift per crossing	0.04
Repetition rate [Hz]	15
RF frequency [GHz]	3
RF voltage [MeV]	1500
Particles per bunch [10^{12}]	2
No. of bunches of each sign	2
Peak current $I = eNc/\sqrt{2\pi\sigma_x}$ [kA]	12.8
Avg. current $I = eNc/circum$ [A]	0.032
Horizontal tune ν_x	55.79
Vertical tune ν_y	38.82

There has been a renewed interest in a muon collider, and new studies of the candidate lattices have been carried out by Snopok, Berz and Johnstone [8] and Alexahen and Gianfelice (private communication). This work (Table 2) also included some dynamic aperture studies that provide insight to the needed aperture in the open-midplane dipoles to be studied here. N. Mokhov (private communication) has estimated a beam gap of 250 mm x 20 mm (H x V), based primarily on energy-deposition considerations from previous studies

Table 2 lists a recent design for a muon collider using 10-T dipole magnets of cos(θ) geometry[3]. We use this work as our baseline.

Table 2. Muon Collider Parameters

	Low Emittance	High emittance
Energy [TeV]	0.75 + 0.75 (γ = 7098.4)	
Average luminosity [10^{34} cm^{-2} s^{-1}]	2.7	2
Average bending field [T]	10	6
Mean radius [m]	361.4	500
Number of IPs	4	2
Proton-driver rep. rate [Hz]	65	60
Beam-beam parameter/IP, ξ	0.052	0.1
β* [cm]	0.5	1
Bunch length, σ_z [cm]	0.5	1
Number of bunches/beam, n_b	10	1
No. of muons/bunch, N_μ [10^{11}]	1	11.3
Norm. transverse emittance, $\varepsilon_{\pm N}$ [μm]	2.1	12.3
Energy spread [%]	1	0.2
Norm. longitudinal emittance (m), $\varepsilon_{\|\|N}$	0.35	0.14
Total RF voltage at 800 MHz [GV]	406.6 x $10^3\alpha_c$	5.6 x $10^3\alpha_c$
RF bucket height [%]	23.9	2.4
Synchrotron tune	0.723 x $10^3\alpha_c$	0.1 x $10^3\alpha_c$

Very recently, after the favorable P5 committee report on muon colliders, there has been renewed interest in muon colliders, with the formation of the Muon Accelerator Program to help coordinate this effort. MAP is very interested in the study of superconducting magnets for the collider. Figure 1 in this proposal comes from the study "Muon Accelerator R&D Program: A Proposal for the Next 5 Years" (FNAL Note). On page 6 they quote the results of the P5 report as motivation, and on page 21 define the needed lattice design. The report also discusses magnets for the collider ring (or a neutrino factory ring) and, to quote, "open-midplane dipole magnet R&D to assess the viability of this magnet type for the collider ring".

This is in part what we propose here. To study the feasibility of HTS magnets of at least 10 T for high-field open-midplane dipoles is totally consistent with the goals of MAP. Collider luminosity scales with magnet field strength. Our goal is the study of the magnetic field that may be achieved with HTS magnets and the related mechanical issues with such open-midplane magnets. We will start with the 10 T of the FNAL lattice, and then study fields up to 20 T.

3. Previous Results on Beam-Debris Energy Deposition in the Coils

Decay particles from the circulating muon beams can heat superconducting magnets, triggering quenching; also, the accumulated dose may degrade materials of all sorts: superconductors, insulation and structural members. In an open-midplane dipole magnet the superconducting coils are located so as to dodge all but a small fraction of the decay particles.

N. Mokhov of FNAL studied the heating in a new breed (see next section) of open-midplane magnets for the LHC (Large Hadron Collider) upgrade in dipole-first optics. Its results, presented at PAC'03 [9], include the energy-deposition analysis of Fig. 3 for the OMD presented in PAC'05 [10]. We quote "These peak values are below the estimated quench limit with a necessary safety margin" [9].

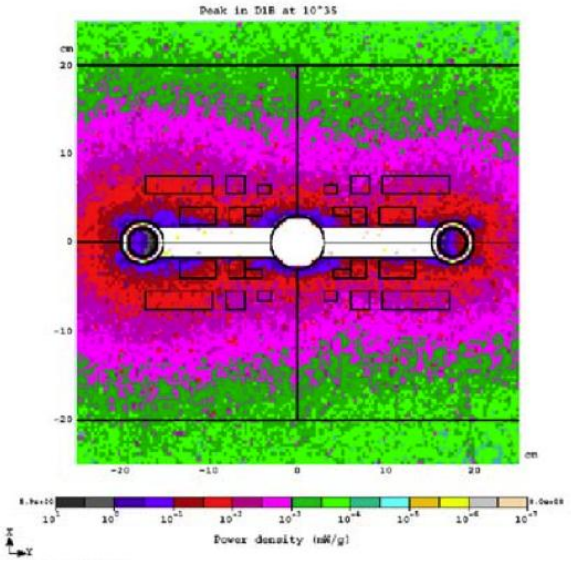

Fig. 3: Heating predicted by Mokhov for OMD for LHC circulating beam [9].

Energy deposition in a muon-collider dipole is similar to that in the LHC dipole-first optics, but the source is different. In the LHC the radiation emanates from the interaction between the two counter-rotating beams; in a muon collider it arises from the decay of the short-lived muons themselves. Muon decay generates debris primarily near the midplane of the muon accelerator or storage ring. According to Mokhov, the open-midplane dipole design should offer benefits in a muon accelerator similar to those in the LHC-upgrade studies, and that "new studies should be made for the muon collider". The PBL team frequently has informal discussions with Mokhov; he is a world expert in calculating the energy deposition from particles transiting materials.

One of the key objectives of this proposed work is to refine predictions of heating in the open-midplane dipoles for the new collider ring lattice; we expect a reduced background in the collider detector as well. This can be studied in Phase II with our same programs.

4. Open-Midplane Dipole

Muons decay rapidly, irradiating nearby matter with energy that can quench a superconductor. A tungsten liner to intercept this radiation and reduce the exposure on the superconducting coils (Fig. 2a) greatly increases the bore, and hence the cost, of the coils. Green, Willen, McIntyre & others [5-7] therefore have proposed to banish conductors from the region most exposed to radiation: near the magnet midplane. However, designs that retain support structure in the midplane to withstand the Lorentz force of attraction between the coils will suffer energy deposition from secondary particles emanating from this support structure. Bonding the coils to the iron (Fig. 2b) to eliminate this cross-midplane structure will not work; the required bond strength is much too great in dipoles of high field.

In the proposed open-midplane design concept (Fig. 4), the coil cross-section in each quadrant is partitioned into inboard and outboard coils, with the outboard coils designed to magnetically attract the inboard coils in the same quadrant with a vertical force sufficient to counterbalance the magnetic attraction from coils on the opposite side of the midplane. The inboard coils therefore need no midplane support material; only the beam tube remains as a secondary-particles source near the coils. Much farther way is the "Warm Target" (see Fig. 4) and, farther still, the support structure for the outboard coils, which attract each other via huge Lorentz forces.

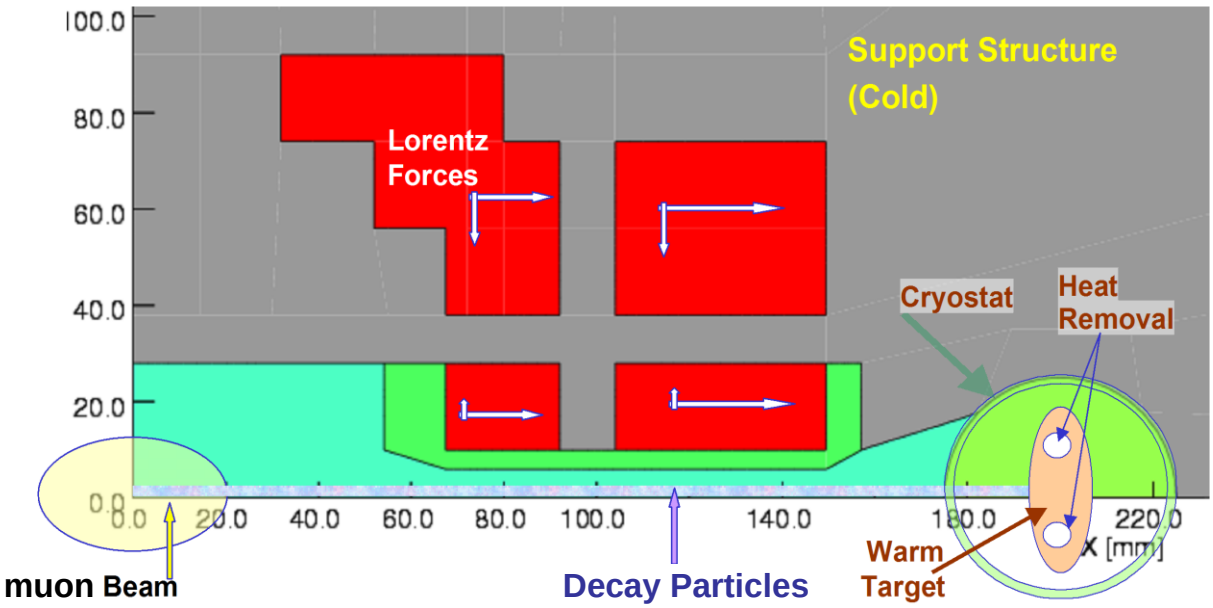

Fig. 4. A truly-open-midplane design, with no midplane structure near the coils to generate secondary-particle radiation.

Dipoles with midplane cold support structure suffer a huge thermodynamic inefficiency in removing heat from the structure. Each watt of heat deposited in a material at 4 K requires approximately 300 watts of wall power for refrigeration. Therefore, it is essential to absorb almost all of the muon-decay energy at room temperature (or at least ~77 K, which consumes ~10 W of wall power for each watt of refrigertion) as in our OMD design. Further arguments against dipoles with midplane structure are that their midplane material may become brittle from the radiation, and their superconducting coils may quench from heating by secondary particles emitted from the midplane structure.

Magnetic, rather than mechanical, support of the inboard coils can allow for a smaller coil gap—the distance between inboard faces of the inboard coils—and improve the field, field quality and overall magnetic design, as for the LHC IR upgrade for "dipole-first optics" [10, 11].

Among the new technical challenges presented by the concept are: a) improving the marginal field quality of the dipoles for the LHC IR upgrade [10, 11]; b) minimizing the peak fields seen by the coils; c) withstanding large vertical forces over a large span; and d) minimizing the heat deposition in the cold region. Phase I has generated considerable evidence for the feasibility of the design, uncovering no "show stoppers" that would preclude a Phase II.

5. High-Temperature Superconductors in Open-Midplane Dipoles

HTS facilitates open-midplane dipole magnets of very high fields. Figure 5 shows the field dependence of critical engineering current density for various wires and tapes at 4 K. HTS is indispensable for any magnet with a peak field much above 20 T.

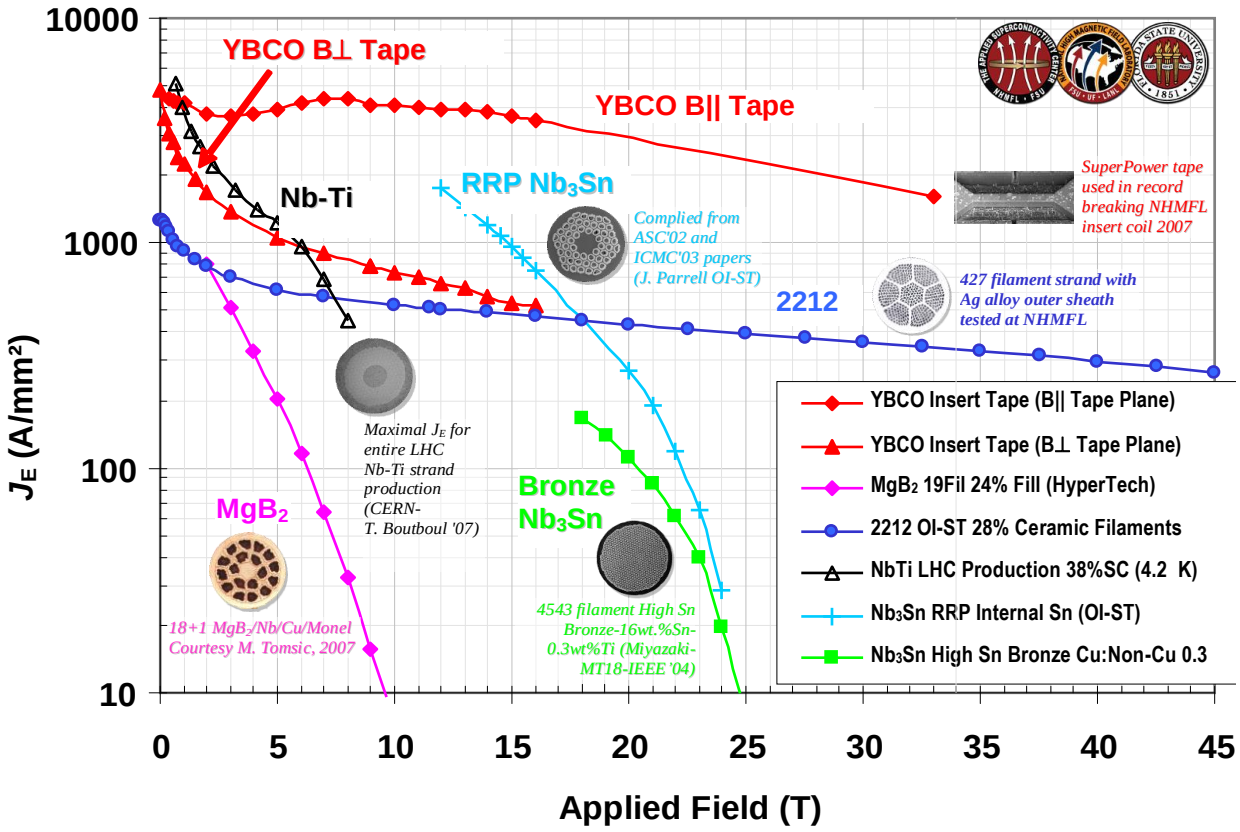

Fig. 5. J_e(B) at 4.2K for different superconductors (compiled by Peter Lee, NHMFL)

YBCO tape is attractive for its outstanding strength and appropriateness for spiral "pancake" coils. Its current capacity degrades only a few percent when bent around a radius of ~10 mm and loaded under tension to ~750 MPa (~0.45% strain). However, its current carrying capacity is dependent on field angle; Figure 5 shows that the critical current of YBCO can differ by nearly an order of magnitude between the most favorable field direction (in the plane of the tape) vs. the most unfavorable direction. This angular dependence of current density complicates the design of magnets that use either YBCO or Bi-2223.

HTS can tolerate heat loads much larger than low-temperature superconductors (LTS). In experiments performed at BNL with an R&D HTS quadrupole for the Facility for Rare Isotope Beams (FRIB) [12], coils 30 cm long remained stable despite a heat load of ~25 W throughout the 35-minute experiment (Fig. 6). HTS also may have a higher radiation tolerance than LTS. Radiation experiments carried out with proton beams at BNL [13] showed that YBCO and BSCCO should not deteriorate appreciably in performance during the desired lifetime (~20 years) of these magnets. This radiation hardness is important for a muon accelerator.

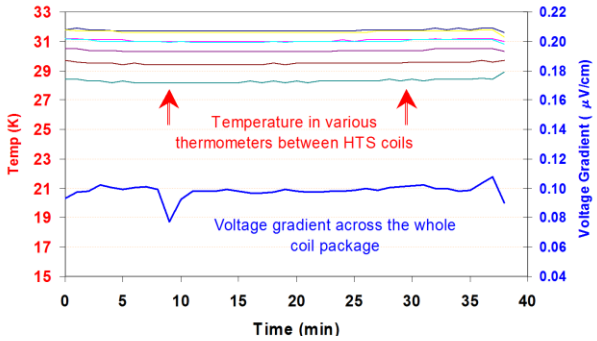

Fig. 6. Left: Heaters between HTS coils. Right: Stable operation at 30 K with 25-W heat load.

To limit the voltage during a quench, the current should be large—several kA or so. Rutherford cable (Fig. 7) of Bi-2212 ($Bi_2Sr_2Ca_2CuO_{8+x}$) carried over 4 kA [14] in coils tested at BNL in 2003; a DOE conductor-development program should raise this value. YBCO might require tapes much wider than the standard 4 mm, or else several tapes in parallel, as in a Roebel cable.

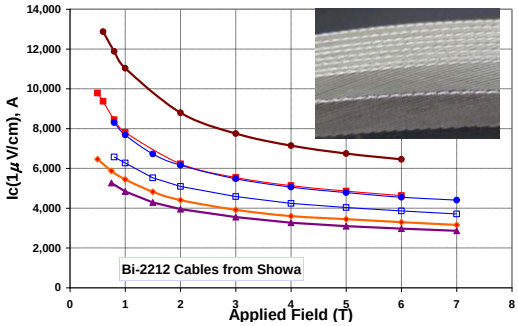

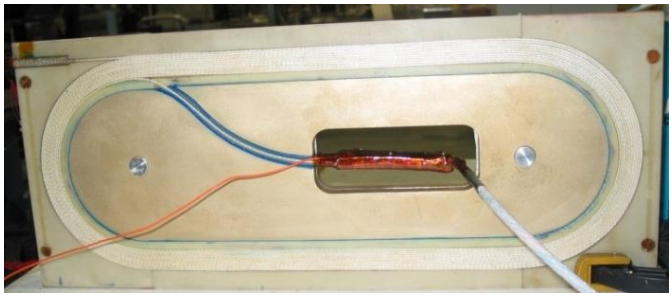

Figs. 7. Left: I_c of 30-strand Rutherford cables made with Bi-2212 wire in a collaboration of BNL, LBNL and Showa. Right: One of several coils built and tested at BNL.

HTS is much more expensive than conventional low-temperature superconductors such as NbTi or Nb_3Sn. However, the elimination of the tungsten liner and consequent reduction in magnet gap should reduce the cost penalty of an open-midplane dipole using HTS. Moreover, HTS should perform more reliably, due to its higher temperature margin. One need not use HTS except where the ambient field and radiational heating are especially high. The much-less-expensive superconductor magnesium diboride (MgB_2) might be appropriate for some coils.

6. Anticipated Public Benefits

6.1. High-Field Nuclear Magnetic Resonance Magnets

NMR (Nuclear Magnetic Resonance) provides valuable information in many fields of science. The frequency of the resonance ώ is proportional to B·M [15], where B is the magnetic field and M is the nuclear magnetic moment. The ability to resolve resonance lines is proportional to at least B^2 [16]. Most experiments use magnets of NbTi, which are limited in field to ~12 T (~500 MHz

proton resonance), even if cooled to superfluid-helium temperature, <2.18 K. Some experiments use pulsed fields, such as the 15 T used by D. Bobela and Taylor [17]. Even magnets of the best low-temperature superconductors, such as $(NbTaTi)_3Sn$, and cooled to ~1.8 K are 5% shy of the 23.5 T considered the holy grail of NMR: 1000 MHz. The few magnets with fields greater than 22.3 T include resistive magnets, with field quality that is marginal, both spatially (field homogeneity) and temporally (field stability). NMR magnets of the highest fields will require superconductors such as Bi-2212, Bi-2223 or YBCO. Known as HTS (high-temperature superconductors), a more appropriate acronym for this application would be HFS (**high-field** superconductors). This SBIR may help to advance magnet technology employing these materials.

We have contacted Mark Bird at the National High Magnet Field Laboratory (NHMFL) for estimates on the market for NMR magnets. He writes "Kevin Smith … says a few years ago the magnet market (excluding the spectrometers) was approximately 100 M British pounds per year. … It is probably best to contact the leading NMR magnet builders: Varian and/or Bruker." Tim Cross writes: "I know of two orders late last fall to Bruker for a total of $23M for NMR spectrometers up to 22.3 T."

There may be a market for HTS magnets of 10-T to 20-T, or operating at a temperature of, say, 35 K to relax cryogenic requirements. Venture capital may be interested in marketing these magnets. Section 7.1 shows that the theoretical field homogeneity can be the $1x10^{-6}$ desired of such magnets. Other issues are: probes of molecular structure; [15], spectra of NMR in liquids [16, 18]; NMR studies on solids [19]; two dimensional NMR studies [19]; and medical imaging.

6.2. Open-Midplane Dipoles for MRI Applications

A conventional MRI uses a solenoid. An open-midplane dipole allows for a different type of MRI whose separation gap might be useful for reducing patient claustrophobia and for physician access for visual examination, sophisticated diagnostics or even surgery. The region of field homogeneity can be very elongated—appropriate for whole-body imaging. We will consult with doctors at the UCLA medical school during Phase II to assess the potential value.

6.3. Federal Government Benefits

The mystery of the neutrino is of key interest to scientists and the U.S. government—especially the DOE. That different flavors of neutrinos can transform into each other has caught the interest of physicists. Their research could benefit greatly from a $\mu^{\pm}$ neutrino factory that sends a beam over 2,000 km. Open-midplane dipoles could be key to the feasibility of such a facility.

They could also be key to a $\mu^+ \mu^-$ muon collider to study a scalar particle that could hold the key to the origin of CP violation and the prevalence of matter over antimatter in the universe. The Director of FNAL (Fermi National Accelerator Laboratory) has stated that there is interest in a muon collider in the long-term future of FNAL. The P5 committee recently endorsed the study of other types of lepton colliders beyond the International Linear Collider (ILC). The magnet study proposed here could further the development of 20-T dipoles and of a $\mu^+\mu^-$ collider of 1.5 to 3.0 TeV that could fit on the FNAL site.

A robust/simple system to cool beams using open-midplane dipoles could have other applications, such as ion lasers and even medical applications.

6.4. Homeland Security Protection against Terrorists' Nuclear Weapons

A muon beam is the only known foolproof method to detect U^{235}. There now is funding to study "Advanced knowledge of the physics of a muon source generation including novel acceleration phenomena."

A small acceleration ring that uses HTS magnets to produce 500 MeV protons would facilitate a portable system to survey sites for fissile material. We will keep this in mind while designing dipoles. The ring might be ~2 m in diameter, with a high-gradient accelerator using dielectric. A flip target in the ring produces pions that decay into muons. HTS allows for a high field, and hence a compact ring, and may avoid the complexity of liquid-helium-temperature cryogenics. Such a device might be used for nanotechnology and medical studies as well.

7. Degree to which Phase I has Demonstrated Technical Feasibility

A primary objective of Phase I was to develop a conceptual and preliminary design of high-field open-midplane dipoles appropriate for a muon accelerator or collider and to confirm that there were no "show-stoppers" that would preclude a Phase II. The preliminary design had: a) good field quality (~0.01%); b) magnetically-supported inboard coils; c) an unobstructed channel to an energy-deposition warm absorber far from any coils; d) acceptable stresses and deformations at a central field of at least 10 T; and e) the potential for substantially higher fields with HTS and the stress-management techniques proposed for Phase II.

Phase I also predicted the energy deposition—both energy density and integrated power—for a variety of coil and absorber geometries. Phase II proposes to continue these energy-deposition simulations in order to refine parameters such as gap width and absorber location to reduce the heat load on the coils.

An R&D plan for Phase II has been developed. This work includes a conceptual design and structural analysis of the coils, support structure and hardware needed to build and test a proof-of-principle test magnet in Phase II.

The work performed in Phase I is summarized in the following sections. This work also forms the basis for the Phase II proposal.

7.1. Design of Open-Midplane Dipole: Equations for Field & Force

To generate designs with optimized combinations of central field B_0, field homogeneity $\Delta B/B_0$, peak-field ratio B_{max}/B_0 and conductor volume or cost, while guaranteeing that the vertical magnetic force F_y on each inboard coil will attract it away from the magnet midplane, analytic equations may be preferable to finite-element methods (FEM) to compute the fields and forces. For a bar of infinite length, rectangular-cross section and carrying a uniform current density J, the vertical field B_y is [20]:

$$B_y = -\mu_0 J \iint \frac{x\, dy\, dx}{x^2 + y^2} = \sum_{i=1,j=1}^{i=2,j=2} (-1)^{i+j}\, c_B\, v_j\, \ln(u_i^2 + v_j^2) + 2v_j \tan^{-1}\left(\frac{u_i}{v_j}\right),$$

where $c_B = \mu_0 J$, and u_i and v_j are shorthand for $a_i - x$; and $b_j - y$, the horizontal and vertical distances, respectively, from a corner $[a_i, b_j]$ of a bar cross section to the field point $[x, y]$. B_x is of the same form, with u_i and v_j interchanged.

This SBIR provided the motivation to derive corresponding equations for the horizontal and vertical components of force, F_x and F_y, between two parallel bars of conductor and to incorporate the formulas into computer programs. The equation for each component of force has sixteen terms. For F_y they are of the form:

$$F_y = c_F\{(3v^2 - u^2)\, u\, \ln(u^2 + v^2) + 2v[3u^2 \tan^{-1}\left(\frac{v}{u}\right) + v^2 \tan^{-1}\left(\frac{u}{v}\right)]\},$$

where $c_F = \mu_0 J_1 J_2 / 6$, and u and v are shorthand for $u_{i,m}$ and $v_{j,n}$, the horizontal and vertical distances between bar corners $[a_i, b_j]$ and $[a_m, b_n]$; i, j, m and n each run from 1 to 2. The equation for the horizontal force F_x is similar, with u and v interchanged.

For muon colliders, cos(θ) dipoles are expensive because the bore needs to be large to accommodate shielding to protect the conductor from radiation from the decaying muons. Open-midplane dipole designs banish windings from the path of this radiation. The design concept proposed here—an outgrowth of R&D for an LHC luminosity upgrade [10, 11]—banishes **structure**, too, from the midplane. Support for the windings closest to the midplane is via magnetic attraction from outboard windings [Fig. 8].

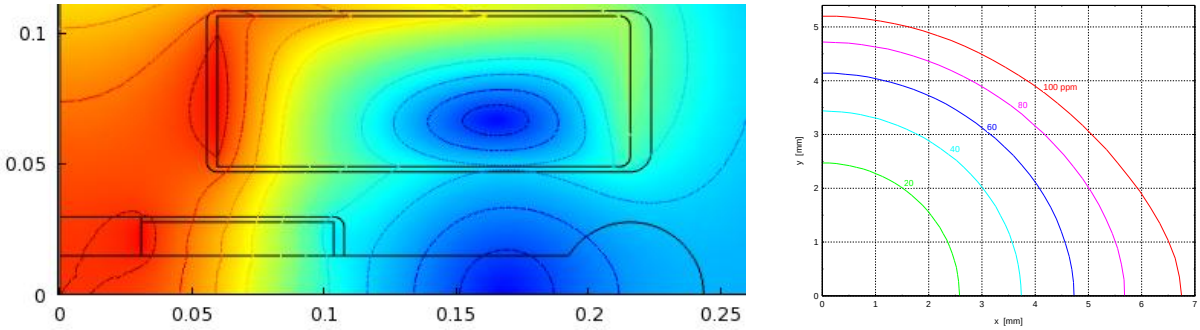

Fig. 8: Simple (two bars per quadrant) OMD of 30-mm -gap. Left: 1st-quadrant windings cross section & field magnitude $B \equiv (B_x^2+B_y^2)^{½}$ (color & contours). $B_0 \equiv B(0, 0) = 10$ T at 200 A/mm^2; B_{max}/B_0 is only 107%. The muon beam is at [0, 0]. The lobed end of the keyhole accommodates a radiation absorber. Right: Contours of field homogeneity; red curve is $\Delta B/B_0 = 1\text{x}10^{-4}$.

The magnet midplane can be truly open, because the inboard bar of conductor experiences a vertical Lorentz force that is upward—not only in total but on the left and right halves separately, to preclude tipping toward the midplane; the horizontal force is 1,356 kN/m. For the outboard bar the force components are $F_y = -3{,}650$ kN/m and $F_x = 4{,}194$ kN/m.

FEM computations confirm that support structure of sufficient cross section can limit stresses and deformations to acceptable levels with a central field of 10 T [Fig. 9]. The von Mises stress to the right of the keyhole is benign, being compressive. The average tension in the web between the inboard and outboard bars is only ~150 MPa at 10 T; the predicted maximum deformation δ_{max} is less than 0.27 mm. One goal of Phase II will be to minimize stresses and deformations by techniques such as coil partitioning, to increase the feasibility of fields as high as 20 T.

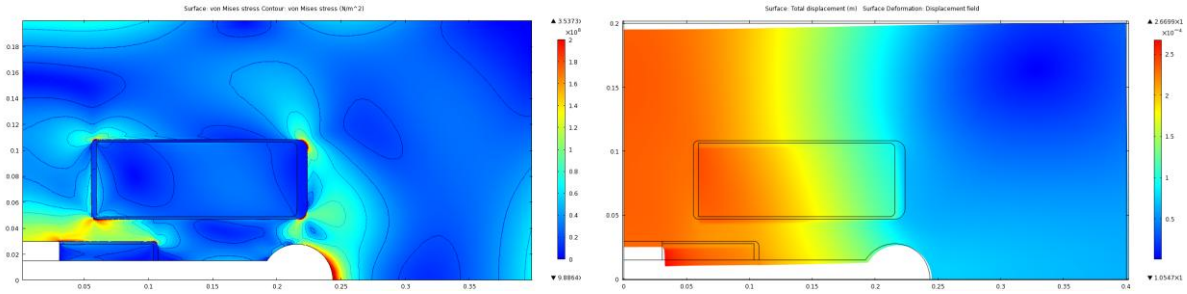

Fig. 9 Stress and strain in OMD of Fig. 8 with support structure x_{max} = 40 cm; y_{max} = 20 cm. Left: Von Mises stress, σ_{vM}. To the right of the keyhole the primary stress is compressive, with a maximum von Mises stress σ_{vM} of 246 MPa. The average tension in the web between the two coils is ~150 MPa. Right: Predicted total deformation, magnified twentyfold.

The open-midplane geometry is amenable to countless variants. For example, Fig. 10 shows a magnet with three conductor bars per quadrant, with field homogeneity of so-called "4th order"—i.e., zero 2nd-order coefficients ∂^2B/dx^2 and ∂^2B/dy^2. Its region of 0.01% homogeneity is four times larger in area than in Fig. 8.

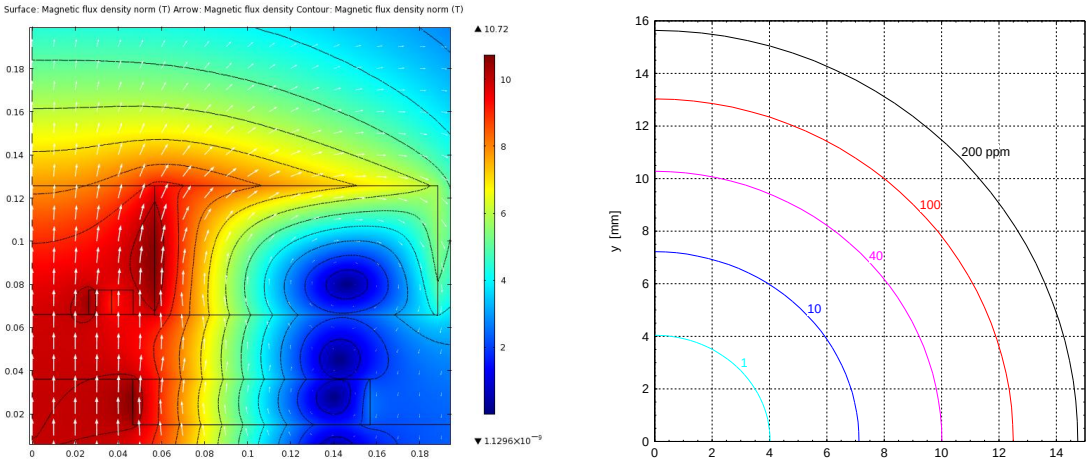

Fig. 10: OMD magnet with three bars per quadrant and $\partial^2B/dx^2 = \partial^2B/dy^2 = 0$; B_0 = 10 T at 200 A/mm^2. As in Fig. 9, the field ratio B_{max}/B_0 is only 107%. Left: Field magnitude (color & contours) & direction (arrows). Right: Contours of field homogeneity $\Delta B/B_0$ in parts per million.

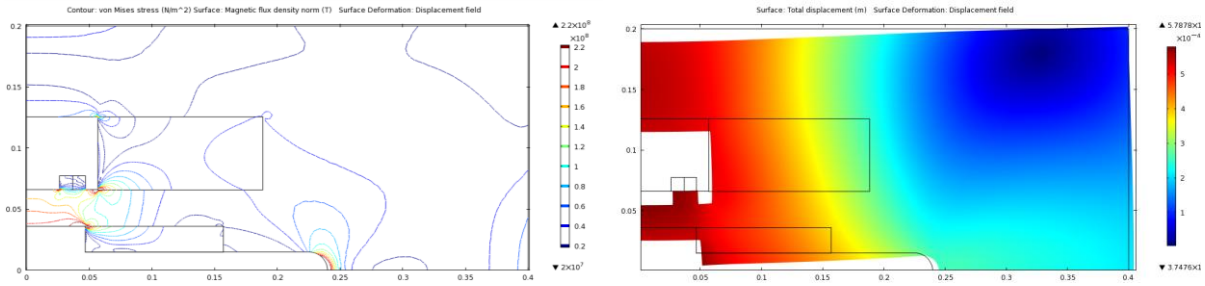

Fig. 11: OMD of Fig. 10. Left: Contours of von Mises stress, σ_{vM}; average σ_{vM} is ~180 MPa in the web at [x = 0; 3.6 cm < y < 6.6 cm]. Right: Total deformation, amplified twentyfold.

The stresses in the web between the windings range up to 180 MPa (26 ksi), even discounting localized stress concentrations; deformations range up to 0.37 mm. Doubling the field to 20 T would quadruple these values. A challenge in pursuing the design of a very-high-field OMD magnet is to limit stresses and deformations to avoid mechanical failure, magnet quenching, and the degradation of field quality. Phase II proposes to address these concerns.

Dipoles are capable—in theory at least—of field homogeneity adequate for magnetic resonance imaging. Figs. 12 & 13 show the conductor-placement in dipole magnets (modeled as infinitely long) with field homogeneity of 1 ppm (part per million) throughout a cross section more than 30 cm in diameter, the standard for thoracic MRI magnets. The magnet of Fig. 13 is of "12th order"; i.e., the leading term in the polynomial expansion of its field is proportional to the 12th power of distance from the origin.

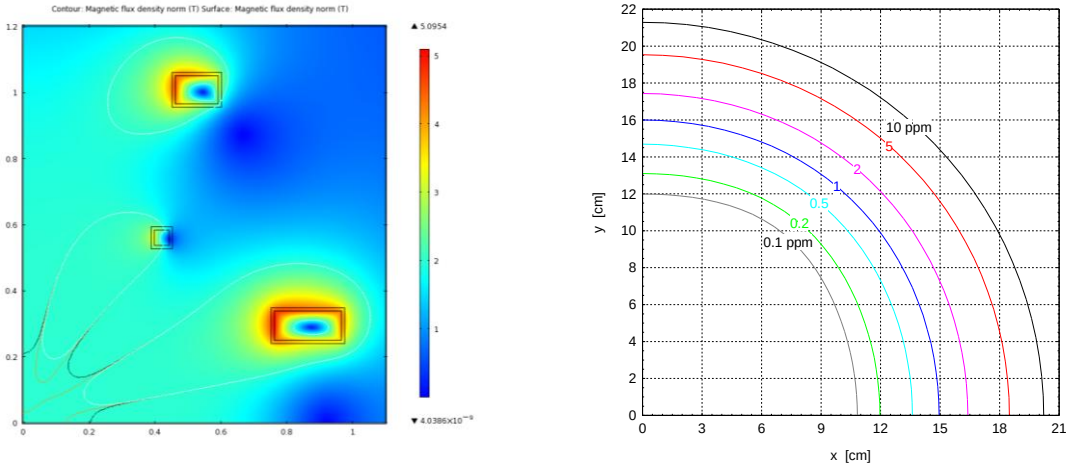

Fig. 12: Dipole magnet with midplane gap and field homogeneity appropriate for MRI. Left: 1st-quadrant coil placement and field magnitude. Distance between inboard faces of inboard coil = 50 cm. B_0 = 2 T. Right: Contours of field homogeneity, from 0.1 to 10 parts per million.

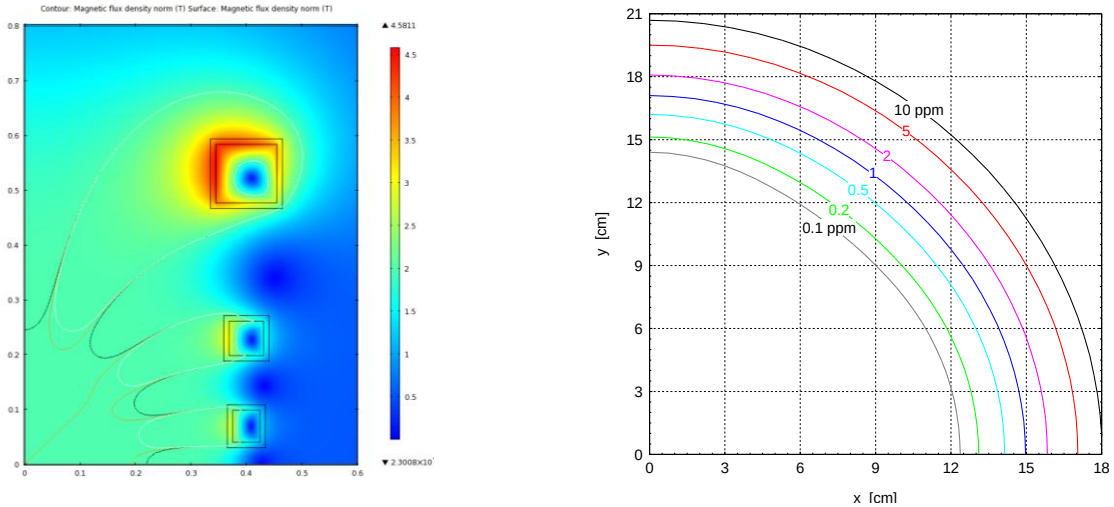

Fig. 13: Compact dipole magnet (no midplane gap) with MRI-quality field homogeneity. Left: 1st-quadrant coil placement and field magnitude. B_0 = 2 T. Right: Contours of field homogeneity.

7.2. Predictions of Energy Deposition and Consequent Temperature Rise

7.2.1. Energy-Deposition Predictions

In a 1.5 TeV center-of-mass muon collider storage ring, muons decay to electrons at a rate of 5×10^9/s per meter of ring. About 1/3 of the muon energy is carried by electrons, which are deflected mostly toward the inside of the ring by the dipole magnetic field. The radiation (energetic synchrotron photons and electromagnetic showers) is ~200 W/m per circulating beam, mostly in the horizontal plane of the storage ring. The energy deposition must not exceed the quench tolerance of the superconducting coils. To predict the energy deposition we use the code MARS15 [21].

Our simulations assume either one unidirectional—or two counter-circulating—muon beams of 750 GeV, with 2×10^{12} muons per bunch at a rep rate of 15 Hz. Figure 14a shows the result for a unidirectional muon beam exiting an open-midplane dipole of 6-m length and 15-mm half-gap. For this example, the peak power density on the inboard bar is 0.13 mW/g on the right (inward) side of the bend and 0.05 mW/g on the left side. For the outboard bar the respective peak power densities are 0.14 mW/g and 0.07 mW/g. These values are within the nominal quench limit of 1.6 mW/g [22].

Note that the tungsten absorber has a slot in its left side (as in Fig. 2b), to reduce backscattering from the absorber. To eliminate backscattering completely it may be possible to remove the right-hand absorber—the one that backscatters more radiation—by completely opening the magnet midplane on its right side, as in Fig. 14b. Preliminary stress predictions suggest that such a design is indeed feasible. We intend to explore this possibility in a more detailed Phase II study.

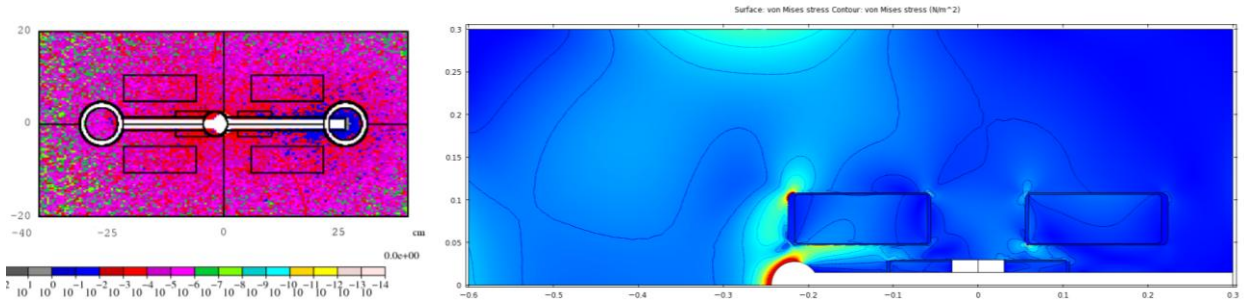

Fig. 14a & b: Left: Energy deposition from a unidirectional muon beam at the downstream end of a 6-m-long open-midplane dipole with half-gap of 15 mm. Right: OMD magnet with structure of "C" shape, without the right-hand absorber, to eliminate its backscattering of radiation onto nearby conductors; maximum σ_{vM} to left of keyhole = 353 MPa.

We first study the energy deposition from the muon beam in the muon collider of the open-midplane dipole specified in the Phase I proposal for a $\mu^+ \mu^-$ collider of 1.5×1.5 TeV. Fig. 15 shows the MARS model of open-midplane dipoles with a) two coils per quadrant (similar to Fig. 9) and b) three coils per quadrant (similar to Fig. 10). This work follows the work of N. Mokhov and S. Striganov from 1996 for a non-open-midplane dipole for a $\mu^+ \mu^-$ collider of 2 TeV on 2 TeV [23].

Our Phase I calculations using MARS [21] give heating estimates similar to Mokhov and Striganov. The major backgrounds come from the decay of μ^- into electrons—or μ^+ into positrons—and other particles. Figure 16 shows the simulated positron energy spectrum, which is consistent with the results of Mokhov and Striganov.

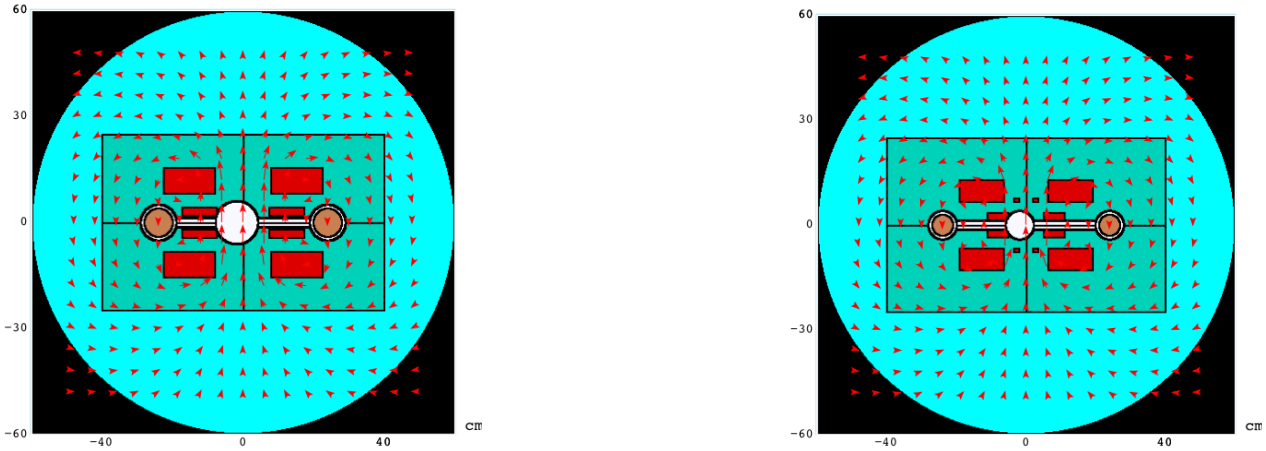

Fig. 15: MARS model of cross section of 6-meter-long open-midplane dipoles and sagitta orbit. Left: Two coils per quadrant. Right: Three coils per quadrant. The red blocks are superconducting coils; the arrows indicate the direction of the magnetic field.

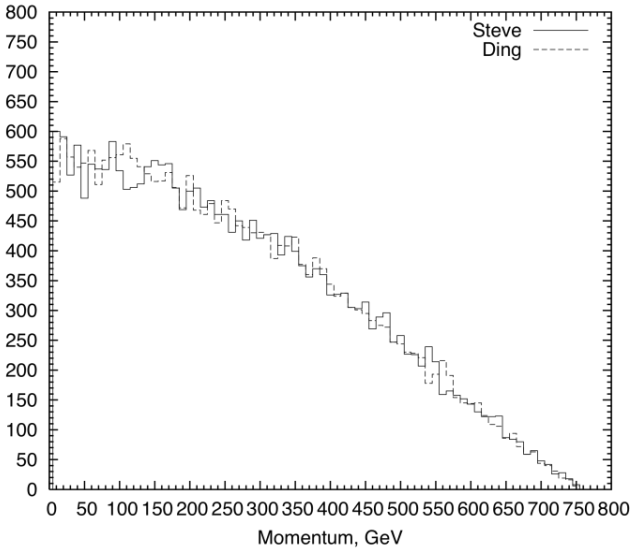

Fig. 16: Positron energy spectrum from decaying muons (50,000 events).

Positrons/electrons from muon decay have a mean energy of ~250 GeV (~1/3 that of the muons). Generated at a rate of 5×10^9/s per meter of ring, they travel toward the inside of the ring and radiate energetic synchrotron photons in the plane of the ring. The positrons/electrons shower to produce not only electrons and photons but also—eventually, and to a much lesser extent—neutrons and other charged and neutral hadrons and even muons, which create high background and radiation levels both in the superconducting coils and in the storage ring. Each muon beam generates~200 W/m of heat. Figure 17 plots the predicted energy deposition.

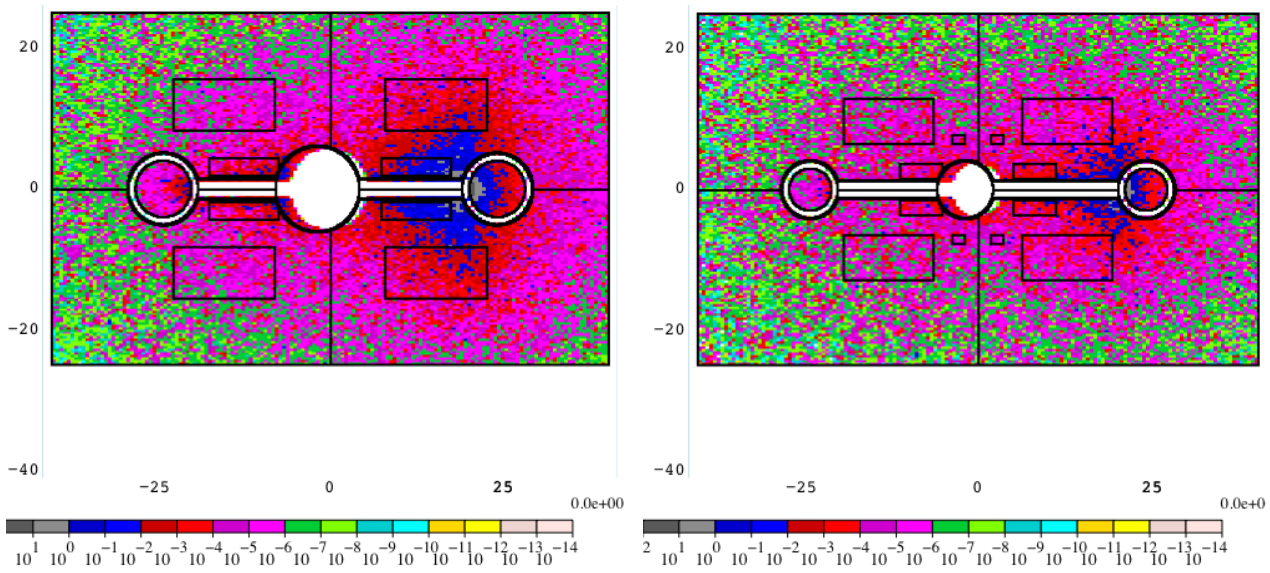

Fig. 17: Energy deposition in dipoles of Fig. 15 at downstream end, where it is expected to be greatest. Left: Two coils per quadrant. Right: Three coils per quadrant.

Figure 3 showed the energy deposition predicted by Mokhov, et al. for an open-midplane dipole for the LHC. Mokhov and Striganov studied the attenuation of azimuthally-averaged energy deposition density in the first superconducting cable shell as a function of the tungsten liner thickness for a cos(θ) dipole and confirmed that thicker liners are better. Similarly, we have calculated the energy deposition for open-midplane dipoles with half-gaps of 15 mm, 30 mm, 50 mm and 75 mm (Figs. 18 and 19).

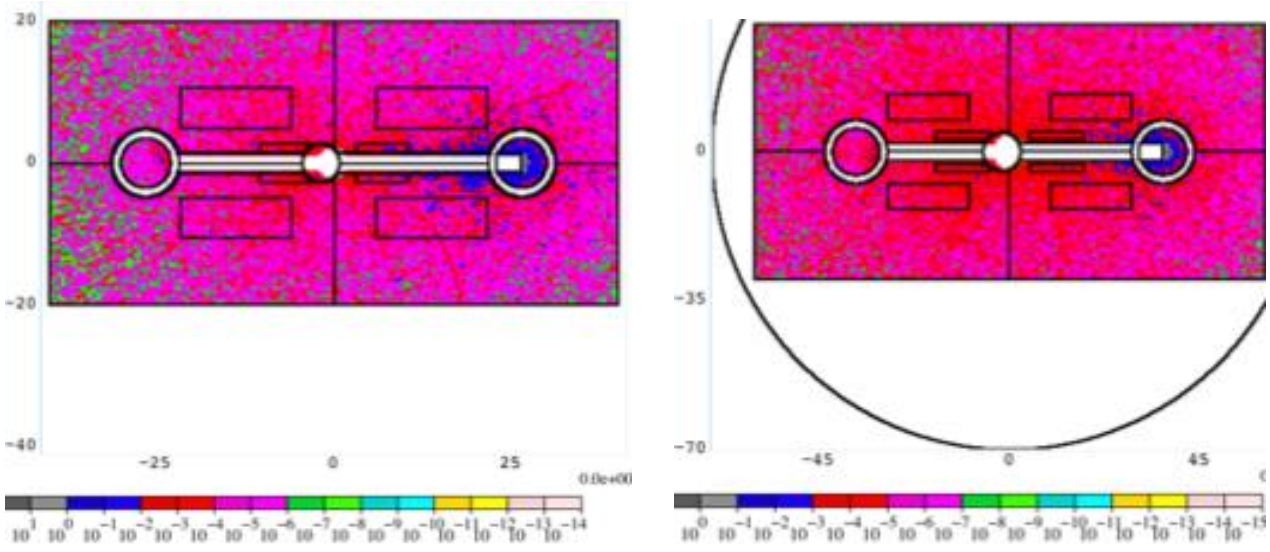

Fig. 18: Predicted energy deposition. Left: Half-gap = 15 mm. Right: Half-gap =30 mm.

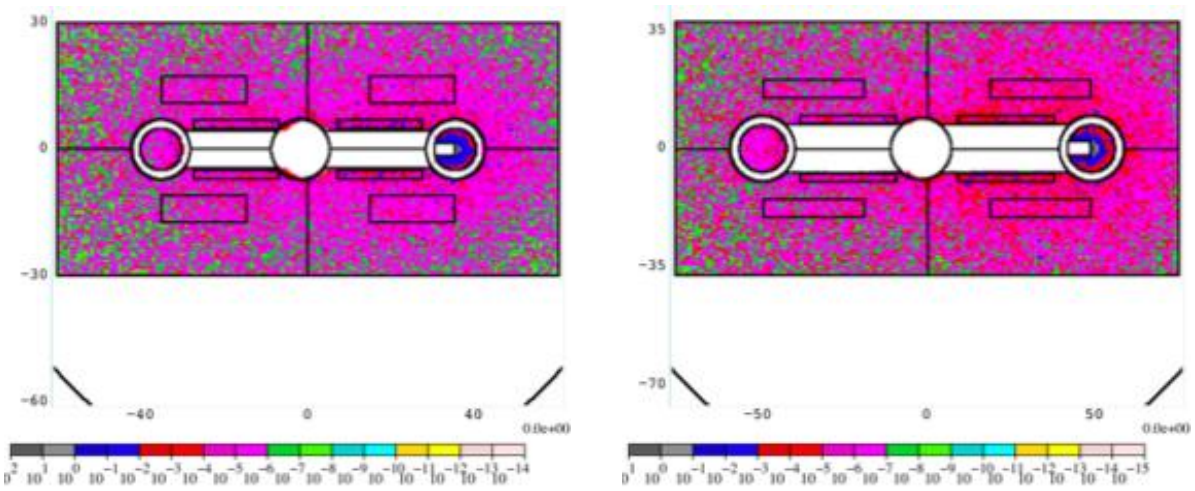

Fig. 19: Predicted energy deposition. Left: Half-gap = 50 mm. Right: Half-gap = 75 mm.

Table 3 lists the peak power density in the inboard and outboard coil in each quadrant. Increasing the gap tends to reduce the maximum energy deposition density, but half-gaps of 50 mm and 75 mm are worse than 30 mm because their tungsten absorbers are too close to the coils and therefore backscatter radiation onto them.

Table 3: Peak Power Density [mW/g] vs. Gap of OMD for Unidirectional Muon Beam

Half-gap height	Inboard coil in Q1/Q4	Inboard coil in Q2/Q3	Outboard coil in Q1/Q4	Outboard coil in Q2/Q3
15 mm	0.06	0.018	0.115	0.105
30 mm	0.009	0.012	0.0028	0.008
50 mm	0.04	0.021	0.0355	0.001
75 mm	0.0175	0.011	0.0065	0.0002

7.2.2. Temperature Rise in Open-Midplane Dipoles from Steady-State Energy Deposition

Equations derived and evaluated for Phase I reveal that at least some of the power-dissipation densities of the previous section are within range of conduction cooling through the stainless steel (Sst) structure surrounding the superconducting bars. The equations model the winding pack and its surrounding Sst as concentric annuli centered on the muon beam. Heat flows radially through each annulus, of thermal conductivity k [W/cm·K], from its inner radius r_i to its outer radius r_o. The power deposition can be a surface heat flux w_s or a power density w_v that may be uniform or nonuniform, decreasing inversely as the 1st, 2nd, 3rd or 4th power of the radius.

For a surface heat flux density, the temperature rise is $\Delta T = c \ln(r)$, where $c = w_s r_i / k$, and r is the normalized outer radius r_o/r_i. For a volumetric power density, the equations are of the form $\Delta T = c F_n(r)$. For a uniform power density, w_v = constant, $F_0 = [r^2 - 2 \ln(r) - 1] / 4$. The remaining equations are $F_1 = r \ln(r) - 1$; $F_2 = \ln^2(r) / 2$; $F_3 = \ln(r) + 1/r - 1$; and $F_4 = [2 \ln(r) + 1/r^2 - 1] / 4$.

Table 4 presents the results for the temperature rise in the Sst from power deposited in the Sst itself. To obtain the total temperature rise in the Sst, one needs to add the contribution from the surface heat flux density w_s at its inner surface from the heat flowing into the Sst from the winding pack. To estimate the total temperature rise in the winding pack one can model it as another concentric annulus of inner radius r_i', outer radius $r_o' = r_i$ and thermal conductivity k'. This contribution to temperature rise is likely to be small, because of the high thermal conductivity of the copper stabilizer that accompanies the superconductor.

Table 4: Power-Deposition Density for 1 K ΔT in OMD's Cooled at Outside of Sst

half-gap, y_{min}	cm	1.500	3.000	5.000	7.500
inboard y_{max}	cm	2.780	4.646	7.113	9.793
inboard x_{min}	cm	3.073	4.690	6.935	9.247
inboard x_{max}	cm	10.36	17.46	27.33	37.90
center of dump	cm	21.58	28.66	35.26	48.90
left edge of dump	cm	19.24	25.11	30.20	42.60
angle to corner	degrees	147.3	139.8	135.3	130.0
core cross section	cm^2	44.5	115	238	473
radius of core	cm	7.53	12.09	17.41	24.54
x_{steel}	cm	20.0	25.0	30.0	37.5
y_{steel}	cm	40.0	50.0	60.0	75.0
$A_{steel} + A_{core}$	cm^2	800	1250	1800	2813
outer radius	cm	31.9	39.9	47.9	59.8
Δr of annulus	cm	24.4	27.8	30.5	35.3
radius ratio	- -	4.24	3.30	2.75	2.44
304 SSt c_k	W/cm·K	0.003	0.003	0.003	0.003
w_v @ i.r.	mW/cm^3	1.00	1.00	1.00	1.00
ΔT with unif. W_v	K	8.84	7.56	6.58	6.47
ΔT if $w_v \sim 1/r$	K	4.51	4.46	4.28	4.47
ΔT if $w_v \sim 1/r^2$	K	2.62	2.87	2.97	3.25
ΔT if $w_v \sim 1/r^3$	K	1.71	2.00	2.18	2.47
ΔT if $w_v \sim 1/r^4$	K	1.22	1.49	1.68	1.94
1K w_v if $w_v = c$	mW/cm^3	0.11	0.13	0.15	0.15
1K w_v if $w_v \sim 1/r$	mW/cm^3	0.22	0.22	0.23	0.22
1K w_v if $w_v \sim 1/r^2$	mW/cm^3	0.38	0.35	0.34	0.31
1K w_v if $w_v \sim 1/r^3$	mW/cm^3	0.59	0.50	0.46	0.41
1K w_v if $w_v \sim 1/r^4$	mW/cm^3	0.82	0.67	0.60	0.51

Table 4 shows that the stainless steel of the open-midplane dipole designs of the previous section will tolerate a power deposition density of ~0.1 to 1.0 mW/cm^3 (~0.015 to 0.15 mW/g) with an allowed temperature rise of 1 K and the Sst cooled only at its outside. For the four magnet designs, the permissible power deposition density values range is 0.11-0.15 mW/cm^3 if the energy deposition is uniform and 0.51-0.82 mW/cm^3 if the power dissipation is localized as $(r_i/r)^4$.

With some difficulty, one can incorporate either copper conduction paths or helium cooling channels into the support structure, to increase the permissible energy deposition density to that permitted by conduction cooling at the external surfaces of the conductor bars.

7.3 Design Studies for Proof-of-Principle Open-Midplane Dipole

The following magnetic and mechanical models develop a preliminary design of a proof-of-principle (PoP) open-midplane dipole whose design is to be refined and then built and tested in Phase II. It is a truly-open-midplane dipole, devoid of material that would backscatter radiation on its way from the beam pipe to a warm absorber beyond the coils.

For economy this novel open-midplane dipole structure is to use coils which are available from other programs or at least can be made with tooling from these programs. This restricts the design; however, we were able to find solutions. For Nb_3Sn coils, the leading candidates are designs from LBL and/or BNL. For HTS coils, we propose to use the coils that are being built for the Facility for Rare Isotope Beams (FRIB).

For the proposed Nb_3Sn PoP open-midplane dipole we considered open-midplane gaps (coil-to-coil separation between the inboard faces of the inboard coils) of 10 mm, 20 mm and 30 mm. In all cases we were able to find coil parameters that guarantee that the outboard coil attract the inboard coil away from the midplane. Thus, magnet designs of large gap are viable. However, the gap of 10 mm (Figs. 20 & 21) gives the best field homogeneity and the highest central field, 9.7 T, and therefore is the leading candidate for the proof-of-principle magnet. The details of the coil geometry will be described in this section, with more details in Phase II.

The FRIB coil (Fig. 22), of high-temperature superconductor, is to generate 1.4 T at 50 K and 5 T at 4 K.

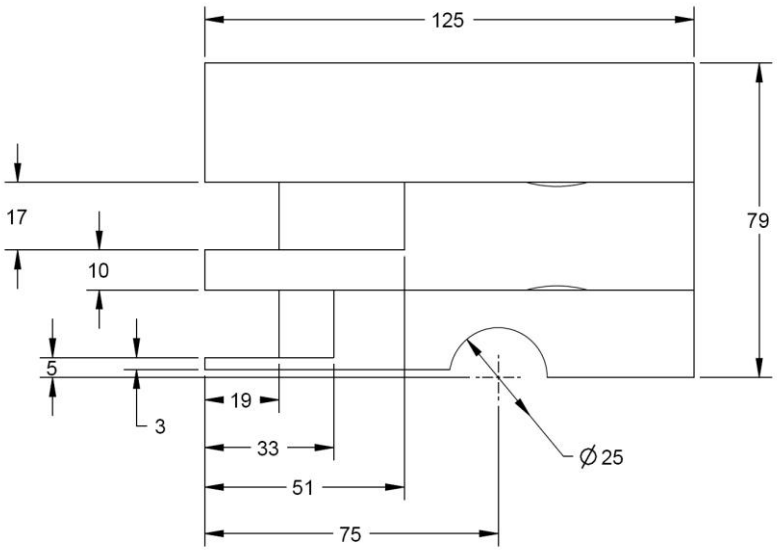

Fig 20. Dimensions of Nb_3Sn coil with coil-to-coil gap of 10 mm and free gap of 4 mm.

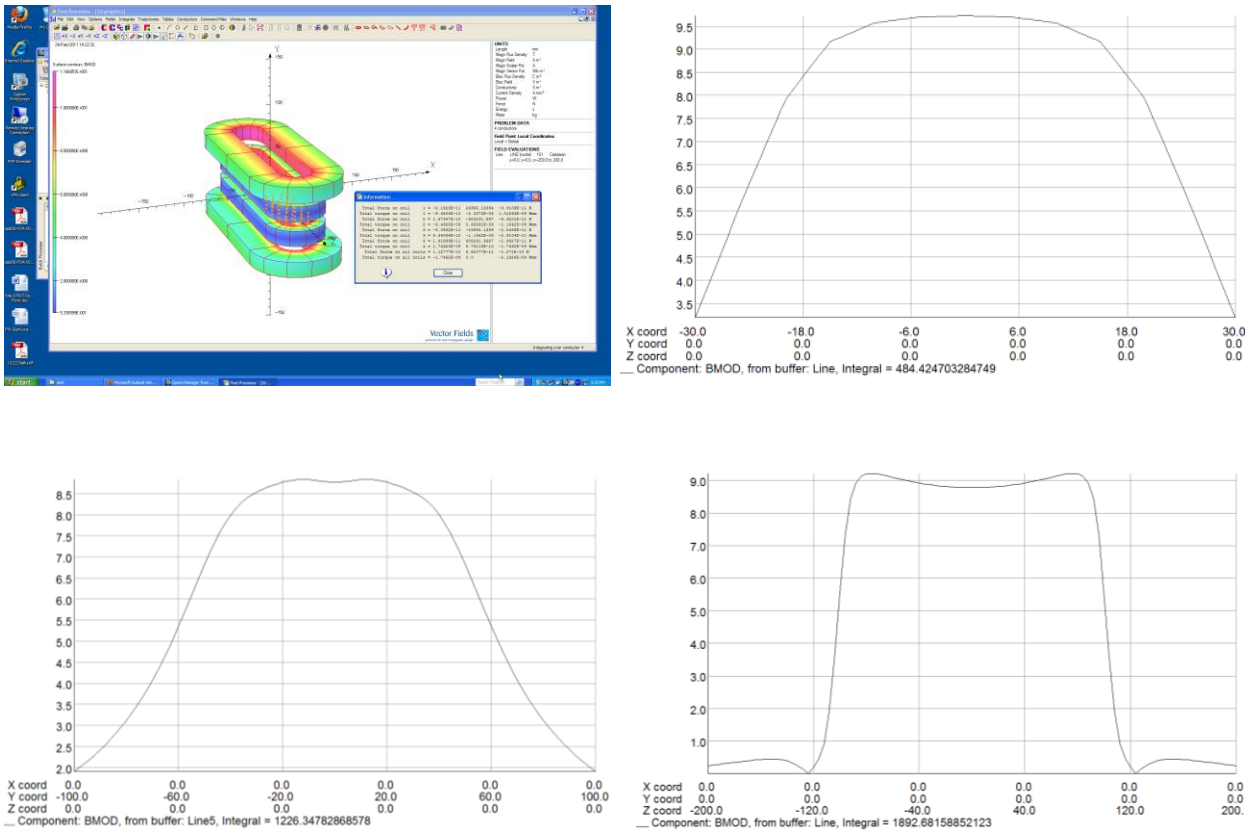

Fig. 21: Nb_3Sn open-midplane dipole with coil-to-coil gap of 10 mm. Top left: Field magnitude, B (color). Top right: B(x). Bottom left: B(y). Bottom right: B(z).

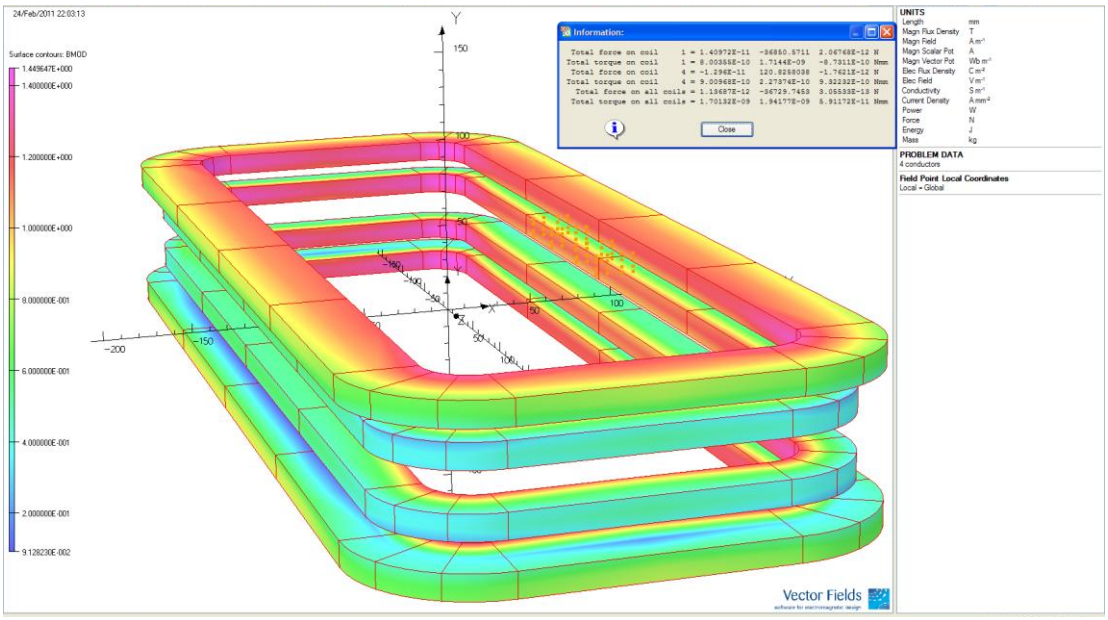

Fig 22. FRIB coil of HTS. $B_0 \approx 1.4$ T at 50 K and ≈ 5 T at 4 K.

7.4. Summary of Phase I Accomplishments

Phase I has advanced the feasibility of open-midplane dipoles for accelerator and storage rings of muon accelerators and colliders. First-order magnetic and structural designs and analytic techniques have been developed to advance the design process. Preliminary energy-deposition predictions—to be refined greatly in Phase II—show promise of adequately limiting the energy deposition in the superconducting coils. The SBIR has generated a candidate design to fabricate and test, for the first time, a proof-of-principle dipole of a truly-open-midplane dipole.

8. Technical Objectives of the Phase II Project

There are three major components to the Phase II proposal. The first component is to develop a more-detailed engineering design of open-midplane dipoles for the accelerator or storage ring for fields of: a) ~10-T dipole (current baseline); b) ~15-T; and c) ~20-T. Higher field increases luminosity.

The second component is lattice and energy-deposition studies for the above three cases. These studies will provide essential feedback to the previous task. The location, geometry, size and temperature of the absorber will be optimized to minimize the energy deposited in the cold mass. This is essential, because the total power from the muon decay is in the megawatt range. A megawatt of refrigeration at 4 K requires ~300 MW of wall power; at 77 K, ~10 MW of wall power; but at room temperature, practically nothing.

The third task—the bulk of the proposal—is to design, build and demonstrate a truly-open-midplane dipole with central field approaching 10 T. This is an ambitious task which has never been tried before and uses a number of innovations that seem to be OK based on the design simulations but have yet to be demonstrated in a real magnet.

8.1 Detailed Design Studies of 10-20 T Open Midplane Dipole for Storage Ring

Open-midplane dipole magnets—like all high-performance superconducting magnets—require sophisticated and thorough analyses: magnetic, structural and thermal. Magnetic analysis addresses issues of field strength and geometry. The goal for the muon-accelerator OMD magnets is field strength of 10-20 T and field homogeneity of 0.01% throughout a cylindrical volume of elliptical cross section with major and minor diameters of perhaps as little as a centimeter or two in typical arc magnets to perhaps ten centimeters or more in magnets for the interaction regions. Magnets for NMR and MRI require field homogeneity of the order of a part per million throughout a volume—typically, but not necessarily, spherical—with a diameter of only a few millimeters for NMR to 30 centimeters or so for thoracic MRI.

Structural analysis is to guarantee that the magnetic stresses—which easily can exceed the yield limit of ordinary structural materials—do not endanger the integrity of the magnet nor generate excessive strains. High-field superconductors are brittle; strain as little as ~0.3% for BSCCO and ~0.5% for Nb_3Sn and YBCO will degrade the critical current. Strain also can degrade the field quality of the magnet. Furthermore, stresses and strains can cause magnet conductors to slide against each other or against surrounding structural material, frictionally heating the conductor and increasing the likelihood of a quench. Structural analysis in Phase II will include stress-management techniques such as coil partitioning to reduce stresses and strains.

Thermal analysis is to refine the very-approximate estimates of Phase I of temperature rises in the magnet conductor, structure and other components and to devise techniques for cooling the magnet and absorber as simply and economically as feasible, with as much heat as feasible extracted near room temperature—and certainly no lower than 77 K—so that the required wall power is not prohibitive because of thermodynamic inefficiency

8.2 Energy Deposition Issues in Phase II:

To protect the superconducting coils in open-midplane dipoles for a c.o.m. muon collider of 1.5 or 3 TeV, we plan to study the following four energy deposition issues: 1) heat load; 2) displacements per atom (dpa); 3) residual dose; and 4) quench stability. Our tasks will include:

1. Model the open-midplane dipole and surrounding materials. Study the energy deposition in fully-open-midplane dipoles of the present Phase I configuration and of a C-shaped geometry.
2. Simulate muon-collider lattice-based backgrounds in the OMD coils. We will consult with the MAP lattice designers to incorporate the latest lattice solutions. An initial design criterion will be 10 T with good field quality in an aperture 100 mm tall by 50 mm wide.
3. Design: a) collimators and tungsten masks between consecutive dipoles; b) liners in the magnetic aperture (wherever needed); and c) thick absorbers to minimize the peak power density of energy deposition in the superconducting coils. The absorber operates preferably at room temperature; the tungsten masks probably are ~10 cm thick with a 5-sigma elliptic aperture.

8.3 Proposed Proof-of-Principle OMD

A major goal of this proposed Phase II SBIR is to fabricate and test a proof-of-principle (PoP) open-midplane dipole with the following features:

1. Magnetic Lorentz forces on the inboard conductors hold them away from the midplane, so that they need no midplane support.
2. The short-sample field should be ~10 T.
3. The conductor is Nb_3Sn, as in a full-size OMD.
4. The OMD incorporates most pertinent cold-mass components—support structure, iron yoke & curout to accommodate a hypothetical warm absorber.
5. The OMD meets all constraints on stress, strain and deformation.

Demonstration of such a magnet will advance both muon collider feasibility and magnet technology, being the first test of a magnet with only magnetic support of the inboard coils. Costs are minimized by using a bolted structure and adopting a proven LBNL Nb_3Sn double-pancake design. The design has a predicted short-sample field of ~9.7 T using Nb_3Sn strands with a critical current density of 2,500 A/mm^2 at 12 T and 4.2 K with a Cu:SC ratio of 1:1; the corresponding current density in the coil is ~750 A/mm^2. Figure 23 sketches the cross section of windings and support structure. End forces are restrained with tie rods and stainless steel plates.

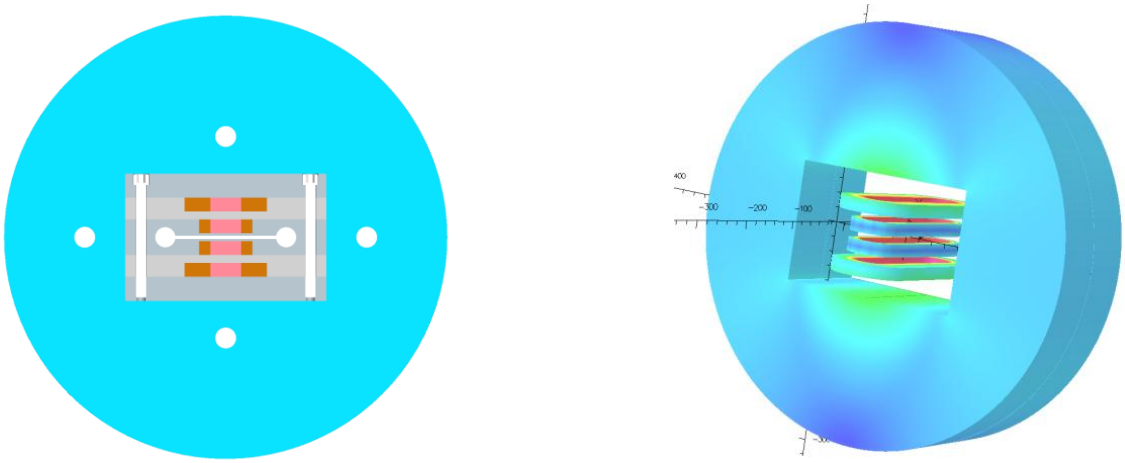

Fig. 23: Left: Cross-section of the proposed PoP OMD. Conductor is brown; coil pole is orange; structure is grey (stainless steel) or blue (iron). The four white circles are for tie rods to restrain end plates that resist end forces. The midplane gap would, in a muon collider, accommodate a beam pipe and, at its dumbbell ends, tungsten absorbers. Right: Field magnitude near racetrack coils & yoke (collar & absorber space omitted for clarity). B_0 = 9.7 T at short-sample current.

Economization limits the size of the coils; field-quality considerations then limit the midplane gap to ~10 mm. Magnets for an actual machine magnet could be much larger in transverse dimensions as well as length and therefore could achieve good field quality with a gap as large as desired (current best guess: 30 mm). This cost-effective subscale PoP should spur further R&D for larger-scale magnets in various laboratories around the world.

ANSYS predictions of stresses and deformations of the coils and support structure will ensure that they are acceptable despite the absence of any cross-midplane bracing between the inboard coils. The preliminary calculations below are for a central field 10% above the short-sample field of 9.7 T in order to give a ~20% margin of safety. More detailed analysis will include stresses and strains within the coils and three-dimensional structural modeling of the ends. Fig. 24 shows that the basic support structure should limit the maximum stress to ~400 MPa, a comfortable value for stainless steel, and the maximum deformation to 87 microns. More importantly, the relative deformation of the coils is only ~20 μm.

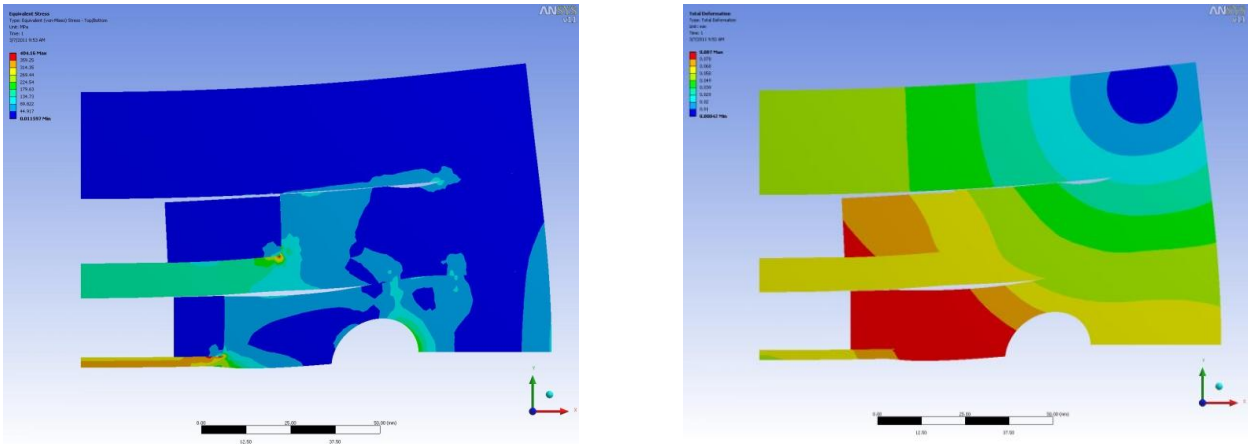

Fig. 24a & b: Left: σ_{vM} at B_0 = 10.7 T, a safety margin of 10% on field and 21% on stress; maximum $\sigma_{vM} \approx 400$ MPa. Right: Deformation δ; δ_{max} = 87 μm; relative δ_{max} of coil ≈ 20 μm.

9. Design, Construction and Test of Proof-of-Principle Open-Midplane Dipole

A key component of this proposal is to demonstrate a truly-open-midplane dipole with a proof-of-principle (PoP) magnet that has no structure at the midplane between the inboard coils. To fit within the SBIR budget, the proposed magnet will be of modest size. However, it is to be of approximately full field and able to test the basic principles of the design. The magnet:

a) needs no structure at its midplane, because its outboard coils magnetically hold the inboard ones away from the midplane;

b) has a short-sample field of nearly 10 T;

c) uses the same conductor (Nb_3Sn) as would a full scale dipole;

d) models many magnet components (support structure, iron yoke, and space for the warm absorber) of the cold mass of a full-scale magnet;

e) satisfies all requirements of a high-field magnet, with acceptable stresses, strains and deformations.

Demonstration of such a magnet will improve prospects for a muon collider and advance magnet technology, because it will be the first with no structure between the inboard coils. This is an ambitious task but one that can be achieved with the plan outlined below.

Phase I has included a preliminary proof-of-principle design of such a magnet and its structure. A more-detailed engineering design of the magnet will be carried out in the first six months of Phase II. The design consists of four coils—two above the midplane and two below. The computed short-sample field is 9.7 T, using Nb_3Sn wire typical in LARP magnets, as discussed earlier.

The design uses a stainless steel support structure and iron yoke and includes space for a warm absorber. The vertical forces on the outboard coils are withstood by 10-mm-thick plates of stainless steel. The space between the upper and lower coils remains structure-free at the midplane from the beam pipe to the cutout for the warm absorber. The horizontal thickness of the support structure and the size of the end plates are chosen to limit the deformation within each coil block to well below the generally-acceptable limit of 50 μm; strains are less than 0.2%.

A low-cost structure is being developed to allow such a demonstration magnet to be designed, built and tested within the proposed budget. Costs are minimized by using a bolted structure, adopting a proven LBNL Nb_3Sn double-pancake small-magnet (SM) coil design [24, 25]. The focus of this PoP is to demonstrate a new magnet geometry, not a new coil technology, and hence it is prudent to use LBNL SM coils, because many coils based on that design have been built and tested (including some at BNL). SM coils have been successfully tested at higher fields and higher stresses in various configurations.

9.1. Quench Protection

Quench protection of the PoP Nb_3Sn coils will be similar to that of the small-scale Nb_3Sn magnet program. The stored energy in this magnet is a modest 60 KJ, and therefore no external dump resistor is required. A full-scale Nb_3Sn OMD with long coils (beyond the scope of this Phase II), would employ quench protection like that being developed for Nb_3Sn magnets for the LARP LHC-upgrade national program, with BNL, LBNL and Fermilab as research partners. Quench protection of HTS is a major challenge, well beyond the scope of this SBIR but being considered by a Particle Beam Lasers Phase II SBIR and several R&D programs at BNL.

9.2. Conductor Parameters

Some key parameters of the conductor and cable for the proposed design are given in Table 5. The specifications for the Nb_3Sn wire require a critical current density of 2,500 A/mm^2 at 12 T and 4.2 K.

Table 5: Key Parameters of the Conductor & Cable for the Proof-of-Principle Design

Critical current density J_{sc}(12, 4.2K), A/mm^2	2500
Copper to superconductor ratio	1
Strand diameter, mm	0.71
Critical current in wire I_w(12, 4.2K), A	495
Number of strands	20
Critical current in cable I_w(12, 4.2K), A	9900
Cable thickness, mm	1.27
Cable width, mm	7.8
Insulation	Fiberglass-epoxy
Overall critical current density, including insulation,	750

9.3. Magnet Parameters

Some key parameters of the proposed design are given in Table 6. The computed short- sample central field of 9.7 T is limited by the 11.9 T peak field at the ends of the magnet; the peak field in the body of the magnet is 11 T. The peak field in the ends and body of the magnets could be reduced with spacers, but for simplicity and reliability this will not be done.

Table 6: Parameters of the PoP Design (Units: mm, T, kN & N/mm)

Bss,	9.7
Bpk(2-D)	11
Bpk(3-D)	11.9
Stored energy [kJ]	60
Amp-turns per quadrant [kA-turns]	584
Turns per quadrant	58
Current/turn [kA]	10
Inductance [mH]	1.2
Lorentz forces, in close collaboration with and guidance	
Fx2D-block1, near midplane	995
Fx2D-block2, away from midplane	1452
Fx2D both	2447
Fy2D-block	61
Fy2D-block2	-545
Fy2D-both blocks	-484
Fy3D-upper coil1	31
Fy3D-upper coil2	-262
Fy3D-both coils upper	-231
Axial forces on one end	
Fz3D-upper coil1 one end	25
Fz3D-upper coil2 one end	46
Fz3D-both upper one end	71
Yoke, o.r.	275
Yoke, inner x	125
Yoke, inner y	85
coil 1 width (double pancake)	17
coil 1 thick	14
coil 1 ss length	152
coil 1 overall length	218
coil 1 turns	18
coil 2 width (double pancake)	17
coil 2 thick	32
coil 2 ss length	152
coil 2 overall length	252
coil 2 turns	40

This PoP is to demonstrate good mechanical integrity (quench performance). The design is not optimized for field quality; however, it is quite good, as was seen in Fig. 21.

For the development and demonstration of a proof-of-principle open-midplane dipole, BNL will carry out the conceptual and detailed magnetic and engineering design of the magnet and support structure, as it did for the LHC Accelerator Research Program (LARP). The design work will be carried out in close collaboration with and guidance from Mr. Weggel (PI of this proposal). Nb_3Sn superconductor and other materials for the coils, support structure and yoke will be purchased directly by PBL and supplied to BNL. BNL will design and fabricate the necessary coil-winding tooling and the coil reaction and impregnation fixtures. Superconductor-related issues (specification, procurement, etc.) will be overseen by Dr. Scanlan (PBL), who is a world-renowned expert in this field. BNL will assemble the magnet and test it at their Vertical Test Facility. At the end of the test, BNL will prepare a report that could be in a form a conference paper.

10. Schedule and Tasks

10.1. Schedule for Refinements to Magnet Design and Study of Commercial Applications

Design a baseline OMD with acceptable field, stresses, strains & ΔT	months 0-3
Predict stresses & deformations in PoP magnet; corroborate BNL results	months 0-6
Research commercial interest in dipoles for NMR, MRI & U^{235} detection	months 0-6
Predict temperature rises in OMD, PoP & other magnets	months 3-18
Pursue feasible dipole designs for NMR, MRI & U235 detection	months 6-18
Refine OMD designs to reduce energy deposition & temperature rises	months 6-18
Document and report results	months 18-21

10.2. Schedule for Energy Deposition Predictions

Establish a baseline OMD magnet configuration	months 0-3
Establish a muon-collider (MC) storage-ring baseline lattice	months 0-4
Incorporate baseline OMD and MC arc lattice into MARS	months 3-6
Evaluate energy deposition in arc lattice elements	months 5-9
Iterate OMD and arc lattice designs with appropriate shielding	months 9-18
Document and report results	months 18-21

10.3. Schedule for Fabrication of Proof-of-Principle Magnet

Magnet design and analysis	months 0-6
Tooling design	months 3-6
Coil parts and tooling fabrications	months 6-10
Coil fabrication	months 9-15
Magnet-part fabrications	months 7-15
Magnet assembly	months 16-18
Cold test	months 18-19
Report preparation	months 20-21

10.4. Tasks for Refinements to Magnet Design and Study of Commercial Applications

1. Develop detailed magnetic design of OMD, based on parameters from Phase I: Weggel & Kirk; supported by Gupta and reviewed by Scanlan & Palmer
2. Refine predictions of stresses and deformations: Weggel
3. Refine predictions of temperature rises: Weggel & Scanlan
3. Investigate commercial applications for OMD's or HTS magnets: Cline, assisted by Weggel
4. Investigate feasibility of OMD or HTS magnets for NMR, MRI & U^{235} detection: Weggel, in collaboration with Cline
5. Document & report results: All

10.5. Tasks for Energy Deposition Predictions

1. Detailed lattice-design work; better specification of field-quality requirements: Garren & Cline, reviewed by Palmer
2. Incorporate an adjacent dipole into the MARS simulation and investigate the energy deposition onto the leading edge of the trailing dipole: Ding & Kirk
3. Install absorbing elements between the two adjacent dipoles in order to mitigate the energy deposition in the dipoles: Ding & Kirk
4. Simulate a 50 m string of the 1.5 TeV collider ring arc lattice to investigate the energy deposition in the 30 m interior segment: Ding & Kirk, assisted by Garren
5. Simulate different OMD models with the goal of reducing the peak energy deposition in the SC coils and the total energy deposition in the 4 K cold mass: Ding, Kirk & Cline
6. Evaluate the dpa rate within the SC coils to predict the operating lifetime of the coils: Kirk
7. Comprehensive prediction of energy depositions and temperature rises: Ding, Cline & Weggel, reviewed by Kirk
8. Document & report results: All

10.6. Tasks for Fabrication of Proof-of-Principle Magnet

1. Design magnetic geometry: Gupta & Weggel
2. Design support structure: Gupta, Anerella, BNL SMD & Weggel
3. Design system to remove energy at a thermodynamically-favorable temperature ($\geq$77 K): Gupta, Weggel & Scanlan
4. Design and build cold mass (test fixture): Gupta, Anerella & BNL SMD.
5. Wind magnet: Gupta, Anerella & BNL SMD
6. React magnet: Gupta, Anerella & BNL SMD
7. Impregnate magnet: Gupta, Anerella & BNL SMD
8. Test magnet at Vertical test Facility: Gupta, Ganetis & BNL SMD
9. Document & report results: All

11. Related Research or R&D; Scientific Goals

11.1. Low-Energy $\mu^+\mu^-$ Colliders

In the model of supersymmetry there will likely be one low-mass Higgs (h_0) and two high-mass (or supersymmetric) Higgs A and H. For the parameter tan ß, larger values lead to a nearly-mass-degenerate system of H and A states, most likely in the 300-500 GeV mass range. Current evidence on SUSY suggests a large value of tan ß. In this case the coupling of H and A to tt and gauge bosons is sharply reduced, making them difficult to produce and study at the Large Hadron Collider or International Linear Collider (ILC).

11.2. High-Energy $\mu^+\mu^-$ Colliders

The FNAL director has approved a long-range plan to study a 1.5-TeV μ^+ μ^- collider. The cooling methods proposed here could be important for this plan. This collider is complementary in all ways to the ILC being planned by the international high energy physics community.

11.3. Muon Source to Detect Weapons of Mass Destruction

A proposal may be submitted to DOD to study a muon source for U^{235} detection, using the magnetic designs determined from this Phase I study, and to design a very compact accelerator. This could become a major commercial activity for PBL, Inc.

12. Principal Investigator and other Key Personnel

Robert J. Weggel will be the PI for this Phase II project. Mr. Weggel has had nearly 50 years of experience as a magnet engineer and designer at the Francis Bitter National Magnet Laboratory at MIT and BNL and as a consultant in magnet design. In the course of his career he has authored over 100 peer-reviewed articles concerning resistive and superconducting magnets as well as hybrid high-field versions. He has had extensive experience optimizing magnets for various uses including solid-state research, accelerator and medical applications. He has assisted D.B. Montgomery in authoring the book "*Solenoid Magnet Design*". Weggel will develop the magnetic and mechanical design of the open-midplane dipole in collaboration with Ramesh Gupta of BNL.

Dr. Alper Garren is a world-renowned expert in lattice design for storage rings and synchrotrons. He performed the lattice design for the FNAL Tevatron and contributed to the design of the SSC and the SLAC B-Factory. Garren will be the lead person in advising and establishing the ring lattice parameters which Ding will incorporate into the MARS model as part of the Phase II work.

Dr. Harold Kirk will join PBL, Inc. part-time upon DOE approval of this Phase II proposal. Dr. Kirk's employment with PBL will be at 20%, time with a corresponding 20% reduction in employment by BNL. Kirk is an internationally-recognized expert on simulating the behavior of elementary particles in particle accelerators. Kirk will engage in energy-deposition calculations and supervise the work of Ding. Kirk will also interact with the PI (Robert Weggel) to make sure that his parameters are correctly included in the calculations.

Dr. Robert Palmer is an internationally-known experimental elementary-particle physicist with expertise in superconducting magnets and the science and applications of particle accelerators. He is a member of the National Academy of Sciences and has won two prestigious APS prizes, the Panofsky for experimental high-energy physics and the Wilson for accelerator physics. He co-discovered the omega minus particle, neutral currents, charmed baryon and direct single photons and invented the free-electron laser. He has been head of BNL's Advanced Accelerator Group and the Center for Accelerator Physics, and Associate Director for High Energy Physics. He is employed 2/3 time by BNL. Palmer will provide general scientific and technical expertise to the Phase II project over its two-year term.

Dr. Ronald Scanlan has had 35 years experience in the field of superconducting magnets and materials at the General Electric R&D Laboratory, LLNL (Lawrence Livermore National Laboratory), and LBNL, serving as group leader and program head. He will assist Ramesh Gupta in the selection of the conductor and evaluate the impact of energy deposition on the conductor.

Ramesh Gupta will be sub-grant PI for the work performed at BNL's Superconducting Magnet Division (SMD). The R&D at BNL will focus on the design, construction and test of the proof-of-principle (PoP) open-midplane dipole. Dr. Gupta will be supported by SMD's M. Anerella, head of the mechanical engineering group, and G. Ganetis, head of the electrical engineering group. Dr. Gupta was key to BNL's lead of the development of the OMD design when it was considered for the luminosity upgrade for the Large Hadron Collider (LHC) in the "dipole-first optics". Dr. Gupta has more than two decades of experience in the design of superconducting accelerator magnets, especially in developing and demonstrating HTS magnet designs and technology for particle accelerators and beam lines. Over the last decade he has developed several innovative designs, such as the common-coil dipole, HTS quadrupoles for the Rare Isotope Accelerator (RIA) and FRIB, low-cost medium-field HTS dipoles, and the current OMD design. He has developed a cost-effective, rapid-turnaround systematic magnet R&D approach that is now being used at BNL, LBNL and FNAL and will be used in this proposal. Dr. Gupta is the PI or sub-grant PI of several HTS R&D grants and of two previous SBIR's with PBL. He is also PI on the development of HTS magnets for RIA and FRIB and sub-grant PI of HTS Superconducting Magnetic Storage (SMES). Dr. Gupta has worked on conventional low temperature superconductor cosine theta magnets for RHIC (Relativistic Heavy Ion Collider) and SSC (Superconducting Super Collider). Dr. Gupta has taught several courses on superconducting magnets at the US Particle Accelerator School.

13. Facilities, Equipment and Resources at Brookhaven National Laboratories

The Phase II project will be administered and coordinated by Particle Beam Lasers, Inc., headquartered in Los Angeles. The company has had several successful SBIR projects in the past 25 years; it currently has three active SBIR's: one Phase I and two Phase II's. The company has the capability, experience and administrative infrastructure to carry out the project proposed.

For work under this proposal, the company plans to subcontract with the BNL Superconducting Magnet Division. Working in collaboration with the PBL PI, the SMD will have responsibility for the design, construction and test of the proof-of-principle open-midplane dipole. The infrastructure (space, tools, test equipment, etc.) that are part of the Division will be made available for the Phase II work. It is difficult to put a value on this infrastructure, but a ballpark number is $1M. This value may be considered an "in-kind" contribution to the project.

BNL has a long history with Nb_3Sn magnets. It was the first laboratory in the world to build Nb_3Sn quadrupoles and dipoles. Those projects were carried out under the supervision of Drs. William Sampson and Robert Palmer; both will participate in this program. BNL currently has a major role to construct Nb_3Sn R&D magnets to upgrade the LHC under LARP. Mike Anerella, who leads the mechanical engineering and construction of that program, will play a similar role here. George Ganetis will supervise electrical engineering and quench-protection work.

The superconducting magnet division has a staff of about 40, including scientists, engineers, technicians and administrative staff. It has been a major player in the development of superconducting magnets for the last three decades. Construction and test of HTS solenoids will be carried out in a 55,000 ft^2 multipurpose R&D complex at the SMD. A prominent asset of the complex is an active cryogenic test facility, complete with high-current, high-resolution and high-stability power supplies. The facility allows a variety of testing of superconductors, coils and magnets from ~2 K to ~80 K. Among the various elements of dedicated equipment in the facility are several computer-controlled, automated coil-winding machines, automated-cycle curing and soldering stations, centralized exhaust-vent systems, and hydraulic presses, all of which are available for use in the construction of superconducting magnetic devices. The building has several large-capacity (>15 ton) overhead cranes. Within the building complex are two machine shops with capacity to manufacture the majority of components needed for the R&D task. BNL has a machine shop and a procurement group to handle orders with private companies.

Figures 25 through 30 give an overview of how the BNL SMD facilities would be used in fabricating the proposed proof-of-principle dipole. Fig. 25 shows a subscale LBNL-type SM-series test coil made at BNL. All coils in the proposed proof-of-principle magnet will be similar to this, and two would be almost identical. Fig. 26 shows a fully-instrumented long Nb_3Sn coil and the computer-controlled winding machine used for an earlier Nb_3Sn coil. Fig. 27 shows two reaction furnaces for reacting Nb_3Sn; one of the two would be used for this project. Fig. 28 shows two vacuum impregnation fixtures (one vertical and one horizontal). Fig. 29 shows a Nb_3Sn 2-in-1 common-coil dipole of 25-mm aperture and 10.2 T field tested in 2006. Fig. 30 shows some current work at BNL on a Nb_3Sn magnet for LARP

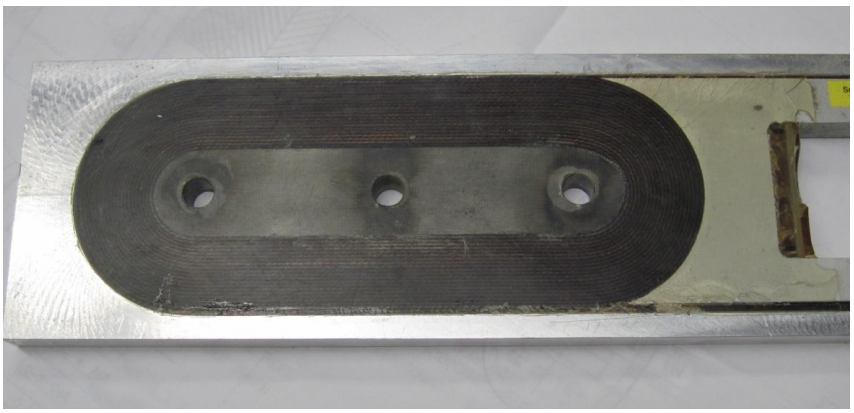

Fig. 25: Sub-scale SM-series test coil (LBNL-type) made at BNL. All coils in the proposed proof-of-principle magnets will be similar to this; two would be almost identical.

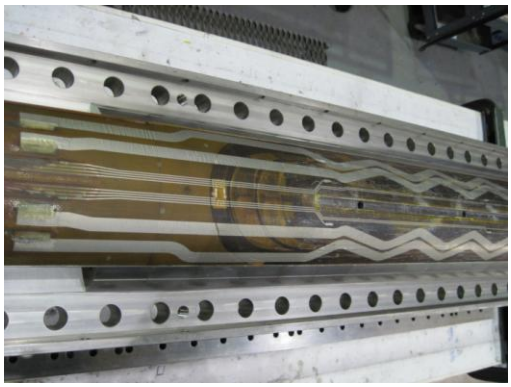

Fig. 26: Left: Fully-instrumented long Nb_3Sn coil at BNL. Right: Computer-controlled coil-winding machine for Nb_3Sn coils.

Fig. 27: Ovens for reacting Nb_3Sn cable and coils. Left: Cubical volume (about 1.1 m^3). Right: Oven for long coils (up to 4 meters). Either oven can be used for the PoP coils.

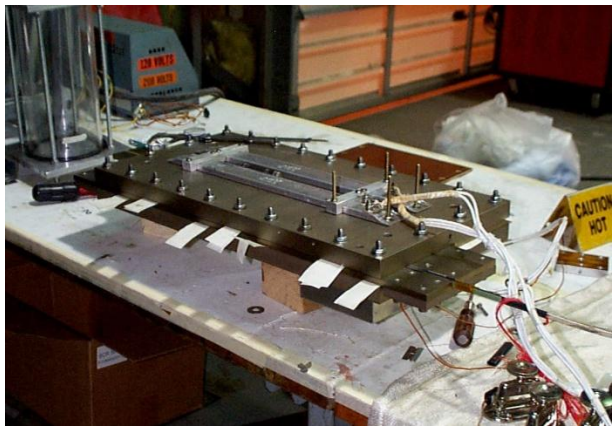

Fig. 28: Vertical and horizontal vacuum impregnation fixtures for impregnating Nb_3Sn coils; either could be modified for vacuum impregnating Nb_3Sn coils for the PoP magnet.


Fig. 29: A 10.2 T Nb_3Sn dipole designed and built at BNL & tested at the Vertical Test Facility.


Fig. 30: 3.4-m-long Nb_3Sn racetrack coil that was wound, cured, reacted and impregnated at BNL. Left: With oven. Right: Being examined by the members of US LARP collaboration.

14. Consultants and Subcontractors

Dr. David Cline is an internationally-known experimental elementary-particle physicist with expertise in the science and applications of particle accelerators and storage rings. He will provide valuable input on physics issues related to the behavior of muon beams through the open-midplane dipole and evaluate such dipoles for other science applications (e.g., LHC upgrade and Homeland Security) and commercial applications (e.g., nanotechnology and medical). He will lead the effort to study a muon collider with HTS dipoles to detect fissile material. A letter of commitment from Dr. Cline is part of this proposal.

BNL will be a subcontractor on this project. As a part of the LHC Accelerator Research Program (LARP), BNL has developed an "Open-Midplane Dipole" design as an option for LHC luminosity upgrade. BNL also has world-class experience with the technologies of high-temperature superconducting coils and racetrack coils, both of which are important to the development of the proposed magnet. The Superconducting Magnet Division at BNL will support the development of the magnetic and conceptual design. Previously-built Nb_3Sn and HTS coils for the common-coil design can be used as part of this proof-of-principle magnet. The certifying official at BNL is Mr. Michael Furey, Manager, Research Partnerships. Mr. Furey's telephone number is 631-344-2103; his e-mail address is mfurey@bnl.gov.

15. Similar Grant Applications, Proposals, or Awards

Particle Beam Lasers, Inc. has no prior, current or pending support for a similar proposal or work.

References

1. http://map.fnal.gov/organization/MAP-Approval.PDF
2. Y.A. Alexahin, et al., "Muon Collider Interaction Region Design", IPAC10.
3. First workshop on Muon Colliders (Napa, CA, 1992), Nucl. Inst. Methods, Vol. A350, pp. 24-56 (1994)

   P. Chen & K. MacDonald, Summary of the Physics Opportunities Working Group, AIP Conference Proceedings, 279, Advanced Accelerator Concepts, 853 (1993)

   Mini-Workshop on mu^+ mu^- Colliders, Particle Physics and Design, Napa CA, Nucl. Inst. Met., A350 (1994), ed. D. Cline

   Physics Potential and Development of mu^+ mu^- Colliders, 2nd Workshop, Sausalito, CA, ed. D. Cline, AIP Press, Woodbury, NY (1995)

   Ninth Advanced ICFA Beam Dynamics Workshop, ed. J. Gallardo, AIP Press (1996)

   Symposium on Physics Potential and Development of mu+ mu- Colliders, San Francisco, CA, Dec. 1995, Supplement to Nucl. Phys. B, ed. D. Cline and D. Sanders.
4. M. Alsharo, et al., "Recent Progress in Neutrino Factory and Muon Collider Research within the Muon Collaboration", Phys. Rev. ST Accel. Beams 6, 081001 (2003)
5. M. Green and E. Willen, "Superconducting Dipoles and Quadrupoles for a 2 TeV Muon Collider", IEEE Trans. on Appl. Supercond., Vol. 7, No. 2, June 1997.
6. P. McIntyre and D. Gross, "m^+ m^- Collider Dipole Concept", Informal Seminar, April 2, 1998.
7. B. Parker, et al., "Magnets for a Muon Storage Ring", PAC'01 (2001).
8. P. Snopok, M. Berz and C. Johnstone, "A New Lattice Design for a 1.5 TeV CoM Muon Collider Consistent with the Tevatron Tunnel," PAC'07, Albuquerque, NM (2007).
9. N.V. Mokhov, et al., "Energy Deposition Limits in a Nb_3Sn Separation Dipole in Front of the LHC High-Luminosity Inner Triple", PAC'03, Portland, USA, May 2003, http://www.jacow.org.
10. R. Gupta, et al., "Optimization of Open Midplane Dipole Design for LHC IR Upgrade," PAC'05, Knoxville, TN, USA (2005).
11. R. Gupta, et al., "Open-Midplane Dipole Design for LHC IR Upgrade", MT-18, Morioka City, Japan (2003).
12. R. Gupta and W. Sampson, "Medium and Low Field HTS Magnets for Particle Accelerator and Beam Lines", ASC, Chicago, August 2008.
13. G. Greene, R. Gupta and W. Sampson, "The Effect of Proton Irradiation on the Critical Current of Commercially Produced YBCO Conductors", ASC, Chicago, August 2008.
14. R. Gupta, et al., "Status of High Temperature Superconductor Magnet R&D at BNL," MT-18, Morioka City, Japan (2003).
15. *Principles of Magnetic Resonance*, 3rd ed., Springer, New York (1996)
16. Becker, ed., *High Resolution NMR Theory and Application*, Academic Press, New York (1980)

17. D. Bobela and Taylor "Nuclear Magnetic Resonance Studies of Tellurium and Antimony Bonding in Crystal Sb_2Te_3 GeTe and $Ge_2Sb_2Te_5$", Jap. J. of Appl. Physics 47, 10, 2008, pp. 8162-8165.
18. Fyfe, *Solid State NMR for Chemists*, CFC Press, Guelph, Ontario (1983)
19. Mehring, M. "High Resolution NMR of Solids", Springer, Heidelberg (1981)
20. D.B. Montgomery, assisted by R. Weggel, *Solenoid Magnet Design*, 2nd printing, pp. 260-271, Krieger (1980)
21. N. V. Mokhov, http://www-ap.fnal.gov/MARS/
22. N.V. Mokhov, et al., "Energy Deposition Limits in a Nb3Sn Separation Dipole in Front of the LHC High-Luminosity Inner Triple", PAC, Portland, USA, May 2003, http://www.jacow.org.
23. N. V. Mokhov and S. I. Striganov, "Simulation of Backgrounds in Detectors and Energy Deposition in Superconducting Magnets at $\mu^+ \mu^-$ Colliders", 9th Advanced ICFA Beam Dynamics Workshop, ed. J. C. Gallardo, AIP Conf. Proc. 372, 1996.
24. D.R. Dietderich, et al., "Correlation Between Strand Stability and Magnetic Performance", IEEE Trans. Appl. Supercond., Vol. 15, no. 2, pp. 1524-1528.
25. R. R. Hafalia, et al., "An Approach for Faster High Field Magnet Technology Development", 2004 Applied Superconductivity Conference.